Article

Concordance between molecular and morphology-based phylogenies of Korean *Enhydrosoma* (Copepoda: Harpacticoida: Cletodidae) highlights important synapomorphies and homoplasies in this genus globally

TOMISLAV KARANOVIC[1,2,5], KICHOON KIM[3,4] & WONCHOEL LEE[3]

[1]*Sungkyunkwan University, College of Science, Department of Biological Science, Suwon 440-746, Korea*
[2]*University of Tasmania, Institute for Marine and Antarctic Studies, Hobart, Tasmania 7001, Australia*
[3]*Hanyang University, College of Natural Sciences, Department of Life Science, Seoul 133-791, Korea*
[4]*Marine Act co., Biodiversity Research Institute, Seoul 133-822, Korea*
[5]*Corresponding author. E-mail: Tomislav.Karanovic@gmail.com*

Table of contents

Abstract

Three new species of *Enhydrosoma* Boeck, 1873 are described from Korea, all found in muddy sediments in the sublittoral zone. They also all have a bifurcate rostrum, just like the type species of this genus, *E. curticauda* Boeck, 1872, and one recently described Korean representative, *E. coreana* Kim, Trebukova, Lee & Karanovic, 2014. These five species share a number of other morphological features, and mostly differ in details of integumental relief, caudal rami shape, and ornamentation of the male antennula. We aim to compare molecular and morphology-based phylogenies obtained for four Korean species of *Enhydrosoma* and two other members of the family Cletodidae: *Geehydrosoma intermedia* (Chislenko, 1978) from Korea and Russia and *Stylicletodes* sp. from Korea. Similar studies in other animal groups have helped to re-evaluate the suitability of morphological characters for reconstructing phylogenetic relationships and taxonomic revisions, and the genus *Enhydrosoma* is considered to be polyphyletic and in urgent need of revision. We use partial sequences of the mtCOI gene for our molecular phylogeny and 32 non-additive characters for our morphology-based phylogeny. High congruence between all cladograms suggests that reconstructing phylogenetic relationships in this group of harpacticoids may be straight-forward, but highlights as homoplastic some morphological characters previously considered important for defining supraspecific taxa in this family. On the other hand, some characters previously overlooked in species descriptions show a significant phylogenetic signal. Even though there is no doubt about the monophyly of the Korean *Enhydrosoma*, their high average pairwise maximum likelihood distances suggest only a remote relationship, and explain their sympatry and/or parapatry. Weak bootstrap support for our basal nodes in molecular phylogenies shows limitations of a single-gene approach, and probably cannot be resolved without a wider taxon and character sampling. Wider taxon sampling will also be necessary to improve bootstrap values of basal nodes in morphology-based cladograms.

Key words: Cladistics, East Asia, mtCOI, phylogeny, sublittoral, taxonomy

Introduction

With more than 60 species described so far (Walter & Boxshall 2015), the genus *Enhydrosoma* Boeck, 1873 is the most speciose member of the family Cletodidae T. Scott, 1905. This family mostly includes active mud burrowers from shallow and sublittoral marine habitats, with some species in the deep sea and brackish waters (Boxshall & Halsey 2004). It is a medium size harpacticoid family with about 115 valid species, classified into 24 genera, and a near global distribution (Wells 2007). However, of the 60 described species of *Enhydrosoma* only about 35 are today considered valid (Kim *et al.* 2014), because many have subsequently been synonymized (Sars 1909; Lang 1948; Por 1986; Fiers 1996) or transferred to other known or newly established genera (Lang 1936; 1948; 1965; Gee 1994, 2001; Gee & Huys 1996; Kim *et al.* 2014). Even after all these taxonomic changes the genus is still not considered a monophyletic group (Gee 1994; Kim *et al.* 2014).

As with many other copepod genera, with the addition of new species the generic diagnosis has been expanded continually to accommodate newly discovered morphological features, with the end result being an extremely heterogeneous group (Fiers 1987; Mielke 1990; Gee & Huys 1996). However, several researchers made notable efforts to redefine this group of species (Sars 1909; Lang 1936, 1948, 1965; Gee 1994, 2001), often as a part of a broader *Enhydrosoma/Cletodes* "clade" of the family, although we are still awaiting a phylogenetic analysis of any sort. One of the main difficulties all researchers faced, which remains true to this day, was that many of the species are known from a very limited set of morphological characters, often with the type material lost or impossible to trace. Gee (1994) re-described the type species, *E. curticauda* Boeck, 1872, and provided a very comprehensive overview of major morphological characters in the whole family. He, however, noticed that the type species has a very isolated position in the genus, and that proper revision may eventually result in *Enhydrosoma* becoming small or even monospecific. Kim *et al.* (2014) described a new species from Korea (*E. coreana* Kim, Trebukova, Lee & Karanovic 2014; which shares many morphological characters with the type species), provided the first molecular data for the family, and erected a new genus for two *Enhydrosoma* species from the North Pacific. They, however, concluded that even after this taxonomic rearrangement, the genus *Enhydrosoma* probably remains polyphyletic, and that further phylogenetic studies and re-descriptions of some poorly described species will be needed before the genus could be revised. Kim *et al.* (2014) provided a re-description of *Enhydrosoma intermedia* Chislenko, 1978, based both on the holotype and newly collected material from Korea and from its type locality in Russia, and described the male of the species.

We report here on three additional new species of *Enhydrosoma* from muddy sediments in the sublittoral zone of Korea, all of which share many morphological features with the type species. They reveal a set of morphological similarities and differences that have not been studied in detail previously. We aimed to compare molecular and morphology-based phylogenies obtained for four currently known Korean species of *Enhydrosoma* and two other members of the family Cletodidae from Korea and Russia, and tried to evaluate the suitability of different morphological characters for reconstructing their phylogenetic relationships. This may help any subsequent revision of this genus globally.

Employing molecular techniques in addition to traditional morphological ones was one of the priorities of this study to aid in species delineation and reconstruction of their phylogenetic relationships. DNA-based species identification methods, referred to as "DNA barcoding", have been widely employed to estimate levels of species diversity, with the 5'end of the mitochondrial cytochrome C oxidase subunit 1 gene (mtCOI) proposed as the "barcode" for all animal species (Hebert *et al.* 2003). The advantage of the mtCOI gene is that it often shows low levels of genetic variation within species, but high levels of divergence between species; for the most common divergence values in a variety of crustacean taxa see Lefébure *et al.* (2006). In recent years several studies on copepods showed that combining molecular and morphological methods can help answer questions related to cryptic speciation (Bláha *et al.* 2010; Sakaguchi & Ueda 2010; Karanovic & Krajicek 2012a; Hamrova *et al.* 2012), invasions of new habitats and colonisation pathways (Lee *et al.* 2003, 2007; Winkler *et al.* 2008; Karanovic & Cooper 2011a, 2012), anthropogenic translocation (Karanovic & Krajicek 2012a), short range endemism and allopatry (Karanovic & Cooper 2011a), suitability of novel micro-morphological characters (Karanovic & Kim 2014a), and definition of supraspecific taxa in conservative genera or families (Huys *et al.* 2006, 2007, 2009, 2012; Wyngaard *et al.* 2010; Karanovic & Cooper 2011b; Karanovic & Krajicek 2012b; Karanovic & Kim 2014b).

Material and methods

Most of our Korean specimens for both morphological and molecular analyses were collected from a number of sampling stations in the sublittoral zone of Gwangyang bay, on the south coast of Korea between 2006 and 2013 (see Karanovic *et al.* 2014). Water depth ranged from 4 to 11 m, and muddy sediments were observed in all stations. First, sediment samples were collected with a van Veen grab sampler with surface area $0.1m^{-2}$ from a small private boat, and then subsamples were collected using acrylic corers with surface area $10cm^{-2}$ for quantitative analysis. The surface layer of sediment was collected using a rice paddle for qualitative analysis. All sediment samples for morphological analysis were fixed in 5% neutralized formalin, and for molecular analysis in 99.9% ethanol. Harpacticoids were extracted from sediment samples using 38 μm sieve and Ludox method (Burgess 2001), and preserved in 70% or 99.9% ethanol (for morphological and molecular analyses respectively). Several Korean specimens were collected from Garorim bay, on the West Coast of Korea, also in muddy sediments and using the same sampling methods as in Gwangyang bay. Russian specimens were collected from Posyet bay (Minonosok inlet) and Russky Island (Rynda bay), using hand-nets (100 μm mesh size) by SCUBA-diving. Water depth ranged from 4 to 7 m, and sandy sediments were observed in all stations (see Kim *et al.* 2014 for more details). Sampling stations data and number of specimens for each new species are given in the Material examined section below.

Most specimens for morphological studies were dissected and mounted on microscope slides in Faure's medium, which was prepared following the procedure discussed by Stock and von Vaupel Klein (1996), and dissected appendages were then covered with a coverslip. For the urosome or the entire animal, two human hairs were mounted between the slide and the coverslip, so the parts would not be compressed. By manipulating the coverslip carefully by hand, the whole animal or a particular appendage could be positioned in different aspects, thus allowing the observation of morphological details. During the examination the water slowly evaporates and the appendages eventually remain in a completely dry Faure's medium, ready for long-term storage. Some specimens were dissected in lactophenol and the dissected parts were mounted on slides using lactophenol as mounting medium or CMC-10. The coverslips were sealed with transparent nail varnish. Some line drawings were prepared using a drawing tube attached to a Leica MB2500 phase-interference compound microscope, equipped with N-PLAN (5x, 10x, 20x, 40x and 63x dry) or PL FLUOTAR (100x oil) objectives. Other line drawings were prepared using a drawing tube attached to an Olympus BX51 differential interference contrast microscope. Specimens that were not drawn were examined in propylene glycol and, after examination, were again preserved in 99.9% ethanol. Specimens for scanning electron micrography (SEM) were dehydrated in progressive ethanol concentrations, transferred into pure isoamyl-acetate, critical-point dried, mounted on stubs, coated in gold, and observed under a Hitachi S-4700 microscope on the in-lens detector, with an accelerating voltage of 10 kV and working distances between 12.3 and 13.4 mm; micrographs were taken with a digital camera and were processed and combined into plates using Adobe Photoshop CS4.

Morphological terminology follows Huys and Boxshall (1991), except for the numbering of the setae of the caudal rami and small differences in the spelling of some appendages (antennula, mandibula, maxillula instead of antennule, mandible, maxillule), as an attempt to standardise the terminology for homologous appendages in different crustacean groups. Only the first new species presented here is described in full. The two subsequent descriptions were shortened by making them comparative. All type specimens are deposited in the collections of the National Institute of Biological Resources (NIBR), Incheon, South Korea.

Specimens for molecular analysis were examined without dissection under a Leica MB2500 compound microscope (objective 63x dry) in propylene glycol, using a concave slide. After examination they were returned to 99.9% ethanol. Before amplification, whole specimens were transferred into distilled water for two hours for washing (to remove ethanol), and then minced with a small glass stick. DNA was extracted from whole specimens using the LaboPass™ extraction kit (COSMO Co. Ltd., Korea) and following the manufacturer's protocols for fresh tissue, except that samples were incubated in the Proteinase K solution overnight, step five was skipped, and 60 instead of 200 μl of Buffer AE were added in the final step, to increase the DNA density. Mitochondrial cytochrome oxidase subunit I (mtCOI) gene was amplified by a polymerase chain reaction (PCR) using PCR premix (BiONEER Co.) in a TaKaRa PCR thermal cycler (Takara Bio Inc., Otsu, Shiga, Japan). The amplification primers used were the 'universal' primers LCO1490 and HCO2198 (Folmer *et al.* 1994). The amplification protocol was: initial denaturation at 94? for 300s; 40 cycles of denaturation at 94? for 30s, annealing at 42? for

120s, extension at 72? for 60s, final extension at 72? for 600s, and the final product was stored at 4?. PCR results were checked by electrophoresis of the amplification products on 1% agarose gel with ethidium bromide. PCR products were purified with a LaboPass™ PCR purification kit and sequenced in both directions using a 3730xl DNA analyzer (Macrogen, Korea). For this study, DNA was extracted and the COI fragment successfully PCR amplified from 14 cletodid specimens (Table 1).

Obtained sequences were checked manually and aligned by ClustalW algorithm (Thompson *et al.* 1994) in MEGA version 6.06 (Tamura *et al.* 2013). The alignment was checked again and all sites were unambiguously aligned. The best evolutionary model of nucleotide substitution for our dataset was established by the Akaike Information Criterion, performed with a jModelTest (Guindon & Gascuel 2003; Posada & Crandall 1998). For the maximum likelihood (ML) analysis the Tamura 3-parameter model (Tamura 1992) was selected, with gamma distribution and assuming that a certain fraction of sites are evolutionary invariable (T92 + G + I). Neighbour joining (NJ) analysis used the Kimura 2-parameter model (Kimura 1980) with uniform rates (K2P). Maximum Parsimony (MP) analysis used complete deletion (gaps/missing data) and TBR search method. All molecular phylogenetic analyses were conducted using MEGA version 6.06 and default parameters. One thousand bootstrap replicates were performed to obtain a relative measure of node support for the resulting trees. Average pairwise ML distances for each dataset were also computed in MEGA version 6.06, using the K2P model. All trees were rooted with *Stylicletodes* sp., which is an undescribed new species from Korea.

Characters for morphological cladistic analysis were coded and optimised using the computer program WinClada, version 1.00.08 (Nixon 2002), and then analysed using NONA, version 2 (Goloboff 1999). No assumption of apomorphy or plesiomorphy was a priori assigned to character states. All analyses were performed with unweighted characters, using the Rachet Island Hopper searches with the following WinClada parameters: 1000 replications; 5 trees to hold; 10 characters to sample; 10 random constraint level; and 'amb-poly = ' (amb-collapses a branch if the ancestor and descendant have different states under same resolutions of multistate characters or of '-'; 'poly =' treats trees as collapsed). Rachet is a method that searches tree space very efficiently by reducing the search effort spent on generating new starting points and retaining more information from existing results of tree searches (Nixon 1999). Bootstrap values were also calculated using WinClada and the Tree-Bisection-Reconnection (TBR) method, with the following parameters: 1000 replications, 10 searches, 100 initial trees (random addition, 1 starting tree per replication, 0 random seed, 100 max trees). We used *Geehydrosoma intermedia* as the outgroup in our morphological cladistics analyses, and included the type species of the genus *Enhydrosoma curticauda* but excluded *Stylicletodes* sp.

Systematics

Family Cletodidae T. Scott, 1905 sensu Por (1986)

Genus *Enhydrosoma* Boeck, 1873 sensu Gee (1994)

***Enhydrosoma apimelon* sp. nov.**
(Figs. 1–9)

Type locality. South Korea, South Sea, Gwangyang Bay, sampling station 10 (see Karanovic *et al.* 2014), muddy sediments, 3455'15.4"N 12747'07.9"E.

Specimens examined. Holotype female (NIBRIV 0000287210) preserved in 70% ethanol. Paratypes: two males and three females (NIBRIV 0000287211) preserved in 70% ethanol; one dissected female (NIBRIV 0000287212) mounted on nine slides; one dissected male (NIBRIV 0000287213) mounted on nine slides; one male and 12 females together on one SEM stub (NIBRIV 0000287214); three males and three females together on another SEM stub (NIBRIV 0000287215); collected on 8 December 2012 by K. Kim. One male and two females used for molecular analyses were collected by K. Kim on 8 December 2012 and 26 April 2012, respectively (see Table 1).

Etymology. The species name derives from the Greek adjective *apimelos,* meaning "slender", "without fat", "lean", and refers to the slender shape of the caudal rami. It was treated as an adjective, agreeing in gender with the neuter generic name.

TABLE 1. List of copepod specimens for which mtCOI fragment was successfully amplified; see text for authors of the specific names. Note: *Stylicletodes* sp. is an undescribed new species from Korea.

Species	Code	Sex	Country	Locality	Station	Coordinates	Date	Bases	GenBank
Enhydrosoma apimelon	20120426_1	♀	Korea	Gwangyang bay	St. 10	34°55'15.4" 127°47'07.9"	26 Apr 2012	660	KT223401
Enhydrosoma apimelon	20120426_2	♀	Korea	Gwangyang bay	St. 10	34°55'15.4" 127°47'07.9"	26 Apr 2012	659	KT223402
Enhydrosoma apimelon	20121208_3	♂	Korea	Gwangyang bay	St. 10	34°55'15.4" 127°47'07.9"	08 Dec 2012	660	KT223403
Enhydrosoma coreana	KC16	♀	Korea	Gwangyang bay	St. 10	34°55'15.4" 127°47'07.9"	30 Jul 2012	660	KJ572386
Enhydrosoma coreana	KC17	♀	Korea	Gwangyang bay	St. 10	34°55'15.4" 127°47'07.9"	30 Jul 2012	660	KJ572387
Enhydrosoma coreana	KC18	♂	Korea	Gwangyang bay	St. 10	34°55'15.4" 127°47'07.9"	30 Jul 2012	679	KJ572388
Enhydrosoma kosmetron	20120726_1	♀	Korea	Gwangyang bay	St. 3	34°53'03.9" 127°39'50.5"	26 Jul 2012	628	KT223404
Enhydrosoma robustum	130422KN_236	♀	Korea	Garorim bay	St. 100A	36°58'32.3" 126°19'17.9"	01 Nov 2012	516	KT223405
Geehydrosoma intermedia	KC35	♀	Korea	Gwangyang bay	St. 13	34°51'09.9" 127°47'27.6"	18 Feb 2012	567	KJ572389
Geehydrosoma intermedia	KC36	♂	Korea	Gwangyang bay	St. 13	34°51'09.9" 127°47'27.6"	30 Jul 2012	663	KJ572390
Geehydrosoma intermedia	KC37	♂	Korea	Gwangyang bay	St. 13	34°51'09.9" 127°47'27.6"	30 Jul 2012	663	KJ572391
Geehydrosoma intermedia	KC39	♀	Russia	Posyet bay	Minonosok	42°36'33.2" 130°51'42.1"	06 May 2012	669	KJ572392
Stylicletodes sp.	KC40	♀	Korea	Gwangyang bay	St. 3	34°53'03.9" 127°39'50.5"	30 Jul 2012	660	KJ572393
Stylicletodes sp.	KC41	♀	Korea	Gwangyang bay	St. 3	34°53'03.9" 127°39'50.5"	30 Jul 2012	660	KJ572394

Description of female. Based on holotype and several paratypes. Total body length, measured from anterior margin of rostrum to posterior margin of caudal rami, from 291 to 335 μm (mean = 309 μm, n = 10). Colour of preserved specimens yellowish; live specimens not observed. Nauplius eye not visible. Prosome comprising cephalothorax with completely fused first pedigerous somite, and three free pedigerous somites; urosome comprising first urosomite (= fifth pedigerous somite), genital double-somite (fused genital and third urosomites) and three free urosomites (last one being anal somite). No sclerotized joint between prosome and urosome. Habitus (Figs. 1A, 2A, 3A) almost cylindrical in dorsal view, widest at posterior end of cephalothorax and tapering posteriorly, boundary between prosome and urosome inconspicuous; prosome/urosome length ratio about 1.3, and prosome only slightly more voluminous than urosome. Body length/width ratio close to 3.5 in dorsal view; cephalothorax only about 1.3 times as wide as genital double-somite. Free pedigerous somites without lateral or dorsal expansions but heavily sculptured; pleurons only partly covering coxae of swimming legs in lateral view. Integument of all somites strongly sclerotized, generally very rough, without discernible cuticular windows or pits, but with characteristic relief of numerous surface ridges and depressions; majority of cuticular depressions and posterior margin of somites covered by dense hair-like spinules, bacterial growth, and detritus, making observation of cuticular pores and sensilla in those regions very difficult. Hyaline fringe of all somites narrow and rough. In addition to hair-like spinules, surface ornamentation of somites and caudal rami consisting of at least two different types of sensilla (slender and bottle-shaped), simple cuticular pores, tubular pores, and few large spinules; exact number of pores and spinules difficult to establish.

Rostrum (Figs. 1B, 3B, E) small, fused to cephalic shield, dorsally recurved in lateral view, bifid at tip, bearing two sensilla between apical horn-like projections, pore located on ventral side; space between sensilla greater than width of one apical horn.

Cephalothorax (Figs. 1B, C, 2H, 3B) tapering anteriorly in dorsal view, about as long as wide; comprising 30% of total body length. Surface of cephalic shield with at least 19 pairs of large sensilla (not counting those on rostrum), of those four pairs along posterior margin on conical mound-looking protuberances and four pairs along lateral margin. Majority of dorsal sensilla in depressions, majority of lateral sensilla on ridges. Interior surface of lateral margin of cephalic shield with characteristic comb of long setules in anterior part (Fig. 2H), touching basis of antenna. Lateral surface of cephalic shield with two large semi-circular depressions, dorsal surface with three central and six paired small and oval depressions; long and strong ridge separating dorsal and lateral depressions.

Pleuron of second pedigerous somite (first free) (Figs. 1A, B, 3A, B) with irregular and shallow relief, posterior margin with at least four pairs of sensilla on conical mound-looking protuberances and row of sparse hair-like spinules; ridge between lateral and dorsal side pronounced but not produced posteriorly; posterior lateral depression large, triangular.

Third pedigerous somite (Figs. 1A, 3A, C) slightly shorter than second pedigerous somite but of similar width; pleuron relief with two smooth dorsal triangles with sensilla on posterior tip, dorso-lateral ridges more pronounced than in second pedigerous somite and slightly produced posteriorly; low laying surface in between triangles and dorso-lateral ridges covered with dense pattern of small, hair-like spinules; posterior margin with at least three pairs of sensilla on conical mound-looking protuberances (in addition to dorsalmost pair on triangles) and row of sparse but long hair-like spinules.

Fourth pedigerous somite (Figs. 1A, 3A, C) similar in size, shape, relief and ornamentation to third pedigerous somite, with slightly more posteriorly produced dorso-lateral ridges and longer dorsal triangles.

First urosomite (Figs. 1A, 3A) slightly longer but not narrower than fourth pedigerous somite; pleuron without free lateral margin; relief similar to that of fourth pedigerous somite but with more pronounced dorso-lateral ridges and smaller and less clearly defined dorsal triangles; posterior margin with at least four pairs of sensilla.

Genital double-somite (Figs. 1A, 2A, C, 3A, 5A) 1.3 times as wide as long in ventral view; completely fused ventrally but with deep dorso-lateral suture indicating original segmentation between genital and third urosomites, thus dividing double-somite into equally long and similarly wide halves. Ventral surface relatively smooth, flat, with shallow relief but dorso-lateral and ventro-lateral ridges pronounced together with pronounced dorsal triangular structures result in almost hexagonal cross-section; dorso-lateral and ventro-lateral ridges significantly produced posteriorly, each bearing single large sensilla on tip. Two additional ventral and two dorsal sensilla visible on posterior margin, and at least three pairs of sensilla visible in anterior half; both anterior and posterior half with ventro-lateral pair of simple pores; posterior margin with row of hair-like spinules, and one ventral row of strong spinules in anterior half, at base of genital operculum. Female genital complex (Fig. 5A) weakly sclerotized

KARANOVIC *ET AL.*

and hardly distinguishable from internal sutures and soft tissue, except large copulatory pore in posterior half and wide copulatory duct; genital aperture ventrally in proximal quarter, covered by reduced sixth legs acting as genital operculum.

Fourth urosomite (third free) (Figs. 1A, 2A, C, 3A, 5A) similar in shape and ornamentation to posterior part of genital double-somite, except narrower and with tubular ventro-lateral pores; posterior projections of ventro-lateral and dorso-lateral ridges long, each with apical sensilla .

Fifth urosomite (preanal) (Figs. 1A, F, G, H, 2A, 5A) shorter and narrower than third urosomite, with shorter posterior projections of dorso-lateral and ventro-lateral ridges, without sensilla, ornamented with pair of ventro-lateral tubular pores, posterior row of long hair-like spinules, and several minute spinules on ventro-lateral ridge.

Anal somite (Figs. 1F, G, H, 2B, G, 3D, 5A, B, C) clefted medially in posterior fifth, with one pair of large dorsal sensilla at base of anal operculum, one pair of lateral tubular pores, one pair of ventral tubular pores, and several stronger terminal spinules. Dorso-lateral and medial corners produced into small serrated flaps; anal operculum (Fig. 3D) semi-circular, long, wide, reaching beyond posterior margin of somite, strongly serrated, representing nearly half of somite's width. Anal sinus (Fig. 1G, H) widely open, with one dorsal and two diagonal rows of long hair-like spinules.

Caudal rami (Figs. 1F, G, H, 2B, G, 3D, 5A, B, C) long, slender, about twice as long as anal somite, widest at base, gently tapering posteriorly, about 3.2 times as long as wide (ventral view), slightly divergent and nearly cylindrical, separated by distance of about ramus width; armature consisting of seven setae (three lateral, one dorsal, three apical). Ornamentation consisting of lateral tubular pore and numerous hair-like spinules on all sides, those on inner margin anteriorly especially long (see Fig. 2B), those on outer posterior corner forming dense tuft (Fig. 1G); dorsal seta (Fig. 2G) smooth, slender, inserted close to inner margin at about first quarter of ramus' length, approximately half as long as caudal ramus, triarticulate at base (i.e. inserted on two pseudojoints); two proximal lateral setae smooth, of equal length, 0.24 times as long as ramus, inserted very close to each other at about two fifths of ramus length, very close to lateral tubular pore. Ancestral distal lateral seta also smooth, only slightly longer than proximal lateral setae, inserted on outer posterior corner of caudal ramus, flanked by tuft of spinules; inner apical seta smooth and very slender, about as long as proximal lateral setae. Principal apical setae fused basally, both without breaking planes and sparsely pinnate; middle apical seta much stronger and longer, about 3.7 times as long as outer apical one and 1.2 times as long as caudal ramus.

Antennula (Figs. 1D, 3E, 6 A–H) short, stout, five-segmented, joined to cephalothorax with small triangular pseudo-segment, approximately half as long as cephalothorax, without cuticular processes, with three rows of strong spinules on first segment. Long aesthetasc on third segment relatively slender, fused basally with adjacent large seta, reaching slightly beyond tip of appendage; even more slender and much shorter apical aesthetasc on fifth segment fused basally with two apical setae, forming apical acrothek. Armature formula: 1.9.7+ae.1.11+ae. Seta on first segment, two setae on second segment, two setae on third segment, and three setae on fifth segment pinnate, all other setae smooth; one pinnate seta on third segment and all pinnate setae on fifth segment recurved, spiniform, with very strong spinules only along convex surface, all other setae slender; six lateral smooth setae on fifth segment biarticulate at base (i.e. inserted on small pseudojoint); dorsal seta on second segment inserted into funnel-shaped depression. Length ratio of antennular segments, measured along caudal margin and from proximal end as:, 1 : 4 : 2 : 0.6 : 4.5.

Antenna (Figs. 2H, 6I) relatively short, composed of coxa, allobasis, one-segmented endopod and one-segmented exopod. Coxa short, with arched row of long posterior spinules. Allobasis longest and most robust segment of antenna, more than three times as long as coxa and about 1.1 times as long as endopod, widest at base and about 2.5 times as long as wide, unarmed, with several long spinules along inner (convex) margin in proximal half. Endopod about as wide as distal part of allobasis, almost cylindrical, about three times as long as wide, with two subdistal surface frills, and two diagonal rows of very large spinules on anterior surface; two strong, pinnate lateral spines flanking minute seta. Apical armature consisting of five elements: two stout but short unipinnate spines, two slender geniculate setae plus massive pectinate spine. Exopod short, forked distally, about as long as coxa but much narrower, with several slender spinules along outer margin, with two apical bipinnate setae; both exopodal setae slender, long, inner seta about 1.3 times as long as outer one, with longer spinules.

Labrum (Fig. 2H) large and complex tri-dimensional structure, trapezoidal in anterior view, rigidly sclerotized, with relatively wide, somewhat convex cutting edge, with subapical row of strong spinules and many apical rows of slender spinules and along posterior surface, additional short row of slender long spinules centrally on anterior surface.

Paragnaths (Fig. 2H) also forming complex tri-dimensional structure, trilobate, with two ellipsoid anterior lobes and one central posterior lobe, all fused at base, all lobes with numerous rows of slender anterior and apical spinules; posterior surface with single transverse row of extremely long spinules.

Mandibula (Figs. 2F, 7H) small, with narrow cutting edge on relatively long coxa, with two strong bicuspidate teeth ventrally, three unicuspidate teeth dorsally, and single dorsalmost slender and smooth seta; dorsalmost tooth longest, ventralmost tooth strongest; dorsal seta slightly shorter than dorsalmost tooth. Palp small, one-segmented, bifurcated distally, proximal half as long and wide as outer branch, inner branch much shorter; proximal part smooth , while each branch with long spinules on anterior surface; inner branch with single bipinnate apical seta, with very strong and long spinules; outer branch with two slender and sparsely bippinate apical setae; all palpal setae slender, subequally long , about 1.5 times as long as palp.

Maxillula (Figs. 1E, 2F, H, 8A) relatively small; praecoxa large, with two outer rows of spinules ; praecoxal arthrite about as long as wide, with two large tube setae on anterior surface and four distal elements (three naked spines and one naked seta), transverse row of spinules on posterior surface. Coxa short, with two distal setae (one pinnate and one naked) and row of spinules on posterior surface; exopod and endopod fused to basis, as long as praecoxal arthrite but much more slender, with six naked setae and row of spinules on posterior surface.

Maxilla (Figs. 1E, 2F, H, 7I) small; syncoxa with three spinular rows on anterior surface and two endites; syncoxal proximal endite with one pinnate stout spine, one slender seta, and one tube seta Syncoxal distal endite similar to proximal endite, except slightly larger and tube seta shorter; basis with short row of spinules and one endite; basal endite with smooth spine distinct at base, tube seta on posterior surface, naked seta and short tubular pore distally.Endopod represented by two tubular setae fused basally.

Maxilliped (Figs. 1E, 2F, H, 8B) prehensile, three-segmented, composed of coxa, basis, and one-segmented endopod. Coxa slender, about twice as long as wide, cylindrical, unornamented, armed with single strong bipinnate seta on inner-distal corner. B basis largest and longest segment, about 2.2 times as long as wide and 1.6 times as long as coxa, with longitudinal row of slender inner spinules, unarmed. Endopod minute, subrectangular, apically with two one short and smooth and one smooth recurved claw; endopodal claw fused to endopod at base, 1.2 times as long as coxal seta and about 1.4 times as long as basis.

All swimming legs (Figs. 1A, 2A) of similar size, long in comparison to body length, composed of small triangular and unarmed praecoxa, large rectangular and unarmed coxa, shorter and nearly pentagonal basis, slender three-segmented exopod, and even more slender two-segmented endopod; none of exopods or endopods prehensile. Pairs of legs joined by simple intercoxal sclerite.

First swimming leg (Figs. 3F, 8C) with smooth, short intercoxal sclerite, distal margin slightly concave. Praecoxa subtriangular, shorter than intercoxal sclerite and about as long as coxa, ornamented with distal row of hair-like spinules on anterior surface. Coxa 2.5 times as wide as long, with longitudinal row of long outer spinules on anterior surface and another inner row of much smaller spinules, both without spinules along distal margin. Basis with one short but strong and finely bipinnate outer spine and one longer and stronger, also bipinnate inner spine, inner spine about 1.4 times as long as outer spine; ornamentation of basis consists of posterior row of very strong spinules, short row of more slender spinules at base of inner spine, and short row of strong spinules at base of outer spine, all on anterior surface. Exopod with all segments of about same length, each about 1.5 times as long as wide and with outer strong and very long spinules and subdistally on anterior surface and more slender spinules along inner margin; first and second exopodal segment each armed with single large outer spine, longer than segment; third exopodal segment with two strong and pinnate outer spines and two slender and very long apical setae; exopodal setae of about same length, 1.6 times as long as entire exopod, and about 2.6 times as long as distalmost exopodal spine, not prehensile, with short outer pinnules and long and sparse inner pinnules. Endopod 0.7 times as long as exopod, also with strong outer and slender inner spinules; first endopodal segment half as long as shortest exopodal segment, about as long as wide, unarmed; second endopodal segment slender, about 5.6 times as long as wide and 4.2 times as long as first endopodal segment, with one strong subapical outer spine, and long apical seta; apical endopodal seta slightly longer than apical exopodal setae, about three times as long as second endopodal segment, and 4.4 times as long as subapical endopodal spine.

Second swimming leg (Fig. 8D) similar to first swimming leg, except for shorter and wider intercoxal sclerite, without inner basal spine, first endopodal segment smaller, and second endopodal segment more slender and armed with two long setae.

Third swimming leg (Fig. 9A) similar to second swimming leg, except for more slender outer seta of basis, and third exopodal segment with additional inner slender seta.

Fourth swimming leg (Fig. 9B) as third swimming leg.

Fifth leg (Figs. 2C, D, E, 6J) biramous, comprising conical exopod and baseoendopod. Exopod longer than endopodal lobe and partly covered by it in ventral view, armed with two outer short spines and one longer apical spine, ornamented with several hair-like spinules and two tubular pores on anterior surface and distal frill on posterior surface. Baseoendopod armed with two inner strong spines, and one apical minute seta fused to several basal spinules, ornamented with numerous hair-like spinules on anterior surface and one long tubular pore at base of each inner spine; apical exopodal spine about 1.2 times as long as proximal endopodal spine, 1.4 times as long as distal endopodal spine, 2.4 times as long as either of outer exopodal spines, and nearly 0.6 times as long as entire exopod.

Sixth legs (Fig. 5A) fused into simple genital operculum, with row of strong spinules at its base; each leg armed with smooth inner seta and unipinnate outer spine; seta slightly longer than spine, both armature elements shorter than some spinules at base of sixth leg.

Description of male. Based on five paratypes. Body length from 288 to 319 μm (mean = 307 μm, n = 5). Genital somite and third urosomite not fused. Habitus (Figs. 3G, 4A), colour, rostrum (Figs. 3H, 4G), shape and ornamentation of cephalothorax (Figs. 3G, H), shape and ornamentation of free prosomites (Fig. 3G), shape and ornamentation of first urosomite (Fig. 3G), general shape in dorsal view and most dorsal ornamentation of other urosomites (Fig. 3G), general shape and armature of caudal rami (Figs. 3G, 4B, 5D), antenna (Fig. 4H), labrum, paragnaths, mandibula, maxillula, maxilla, maxilliped, and all swimming legs (Fig. 4A) as in female. Prosome/urosome ratio about 1.2, greatest width at posterior end of cephalothorax, body length/width ratio about 3.7; cephalothorax 1.5 times as wide as genital somite in dorsal view.

Genital somite (Figs. 3G, 4C, 5D) homologous to anterior part of genital double-somite in female but much narrower compared to other parts of urosome, 1.5 times as wide as long in ventral view, with all sensilla and pores homologous to those in female, no additional sensilla and pores observed; ventral surface without ridges or ornamentation, except spinules as base of sixth leg. Right sixth leg developed into genital operculum, while left sixth leg completely reduced, posterior short row of slender spinules as its only remnant; no spermatophore visible inside any examined specimens.

Third urosomite (Figs. 3G, 4C, 5D) homologous to posterior part of genital double-somite in female but proportionately much narrower, without ventro-lateral cuticular pores, and with ventral posterior row of very strong spinules.

Fourth urosomite (Figs. 3G, 4B, 5D) also narrower than in female, without tube on its ventro-lateral pores, and with medially interrupted ventral posterior row of very strong spinules.

Fifth urosomite (Figs. 3G, 4B, 5D) similar to that in female, only proportionately slightly narrower in ventral view.

Anal somite (Figs. 3G, 4B, 5D) similar to that in female but posterior-medial cluster of spinules not fused together.

Caudal rami (Figs. 3G, 4B, 5D) similar to those in female but longer in proportion to anal somite and generally more elongated; armature and ornamentation as in female.

Antennula (Figs. 3H, 4A, D–F, 7A–G) much longer than in female, almost as long as cephalothorax, strongly geniculate, six-segmented, with geniculation between fourth and fifth segments, without strong spiniform setae; segments in geniculation sclerotized, without cuticular ridges along anterior surface; first two and last to segments clearly homologous to those in female, but all except first two segments with numerous differences in shape and/or armature and ornamentation; second segment also with characteristic dorsal seta in funnel-shaped depression (Fig. 3H) as in female; third segment small, triangular, without clear homology with segments on female, unornamented, with seven slender setae; fourth segment largest and strongest, with continuous row of strong spinules on dorsal surface directed anteriorly (Fig. 3H), with characteristic brush-like organ on anterior surface (Fig. 4E), large aesthetasc as in female, and 11 smooth and slender setae, one of them fused basally with aesthetasc (Fig. 4D). Penultimate segments with single slender seta as in female (Fig. 4E) but significantly more elongated; last segment with distal tip produced into powerful spiniform process (Fig. 4F), another smaller process near midlength, acrothek as in female but displaced to about midlength, six lateral slender setae as in female on pseudojoints, no robust spiniform setae.
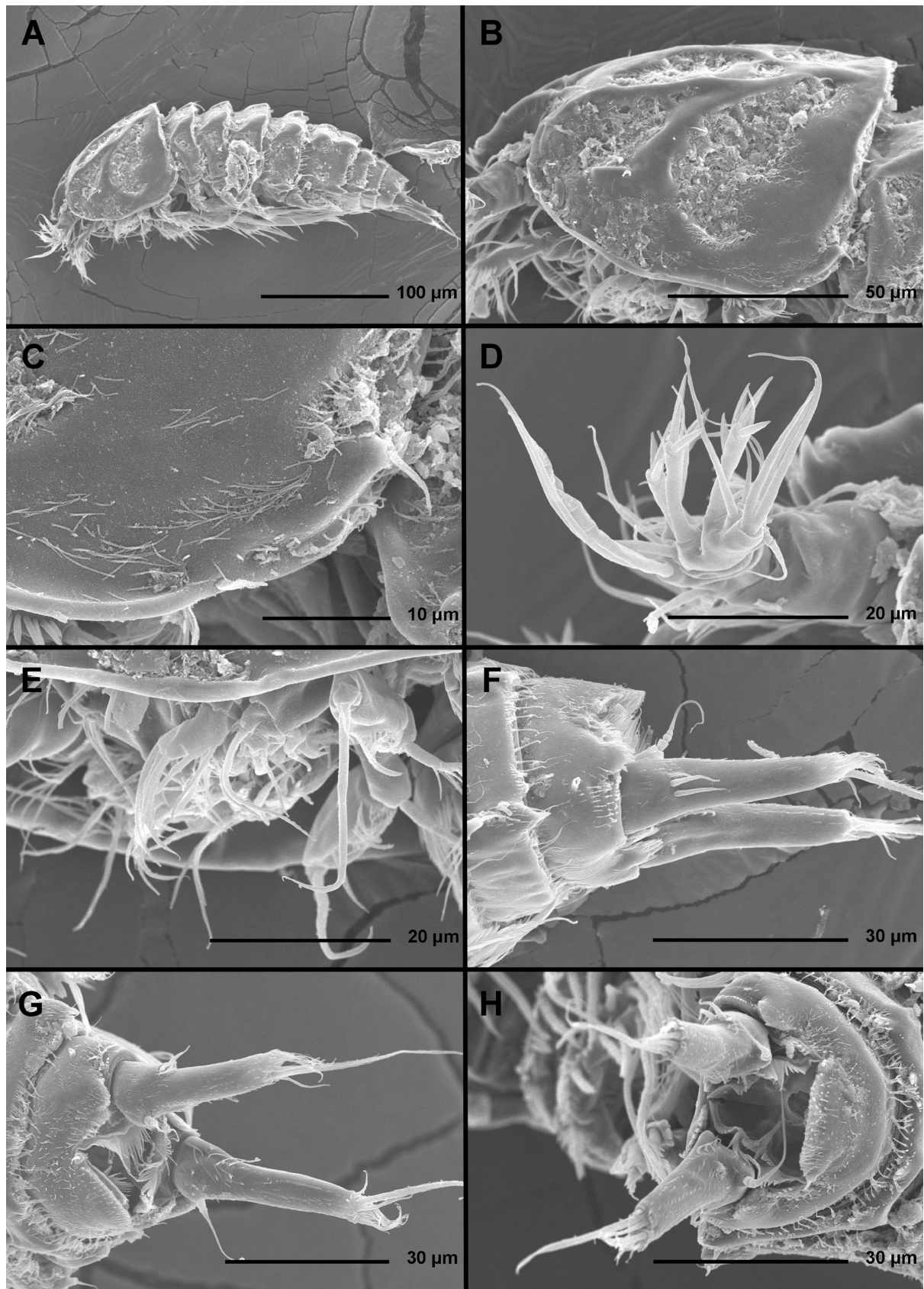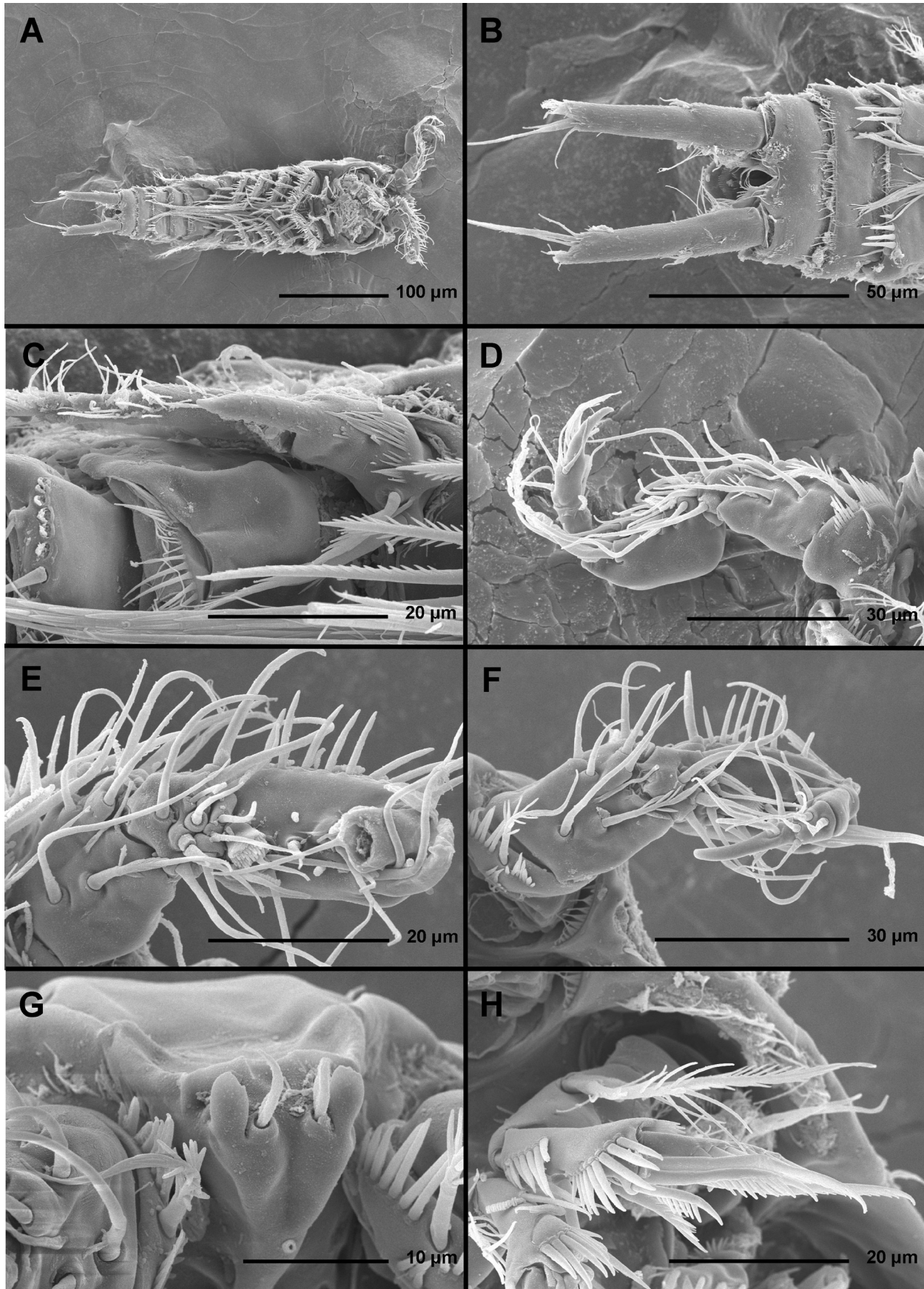
FIGURE 1. *Enhydrosoma apimelon* **sp. nov.**, SEM photographs, A-F, paratype ♀1; G, paratype ♀2; H, paratype ♀3: A, habitus, lateral; B, cephalic shield, lateral; C, posterior-distal corner of cephalic shield, lateral; D, antennula, lateral; E, mouth appendages, lateral; F, anal somite and caudal rami, lateral; G, anal somite and caudal rami, latero-posterior; H, anal somite and caudal rami, posterior.
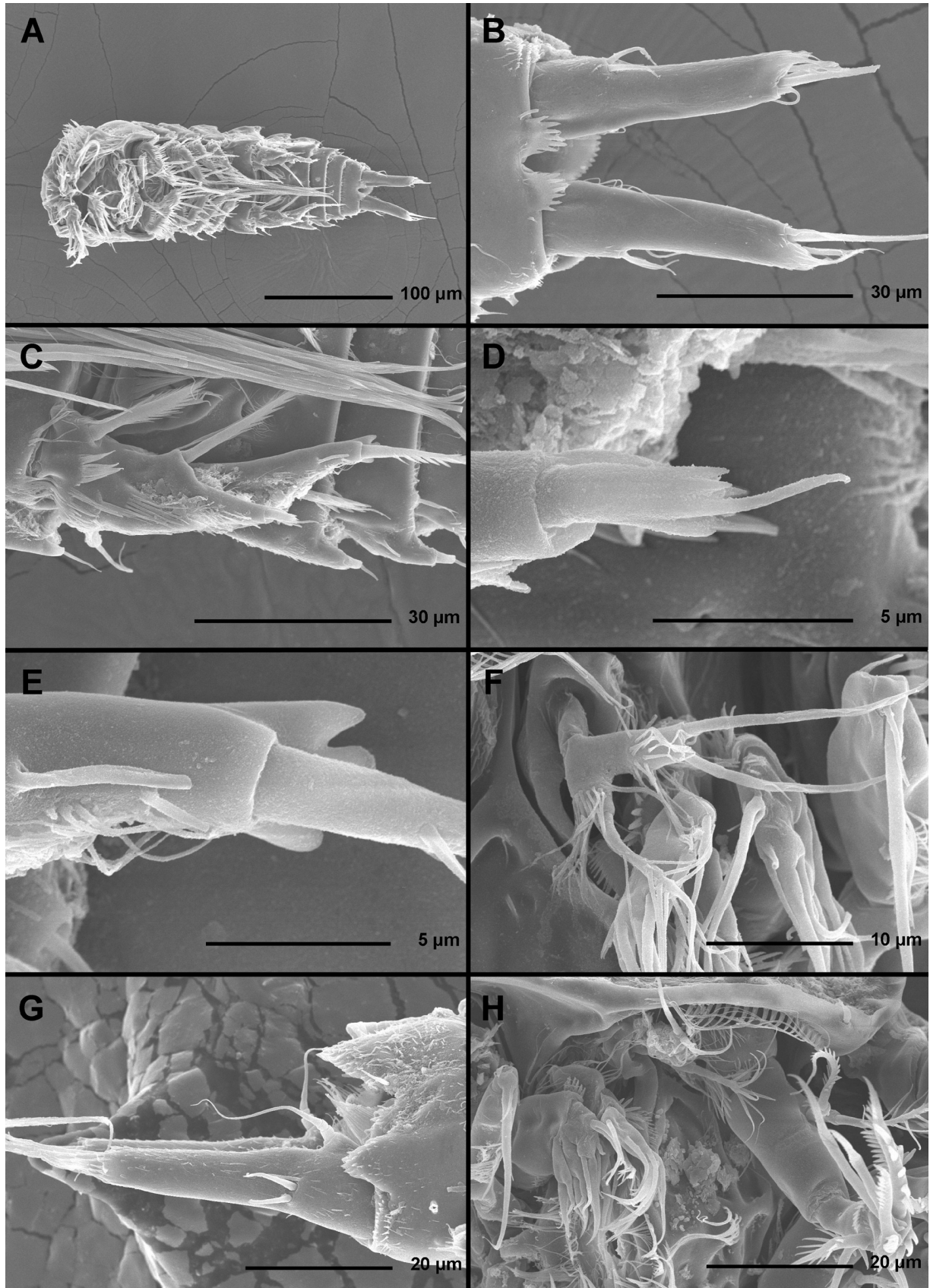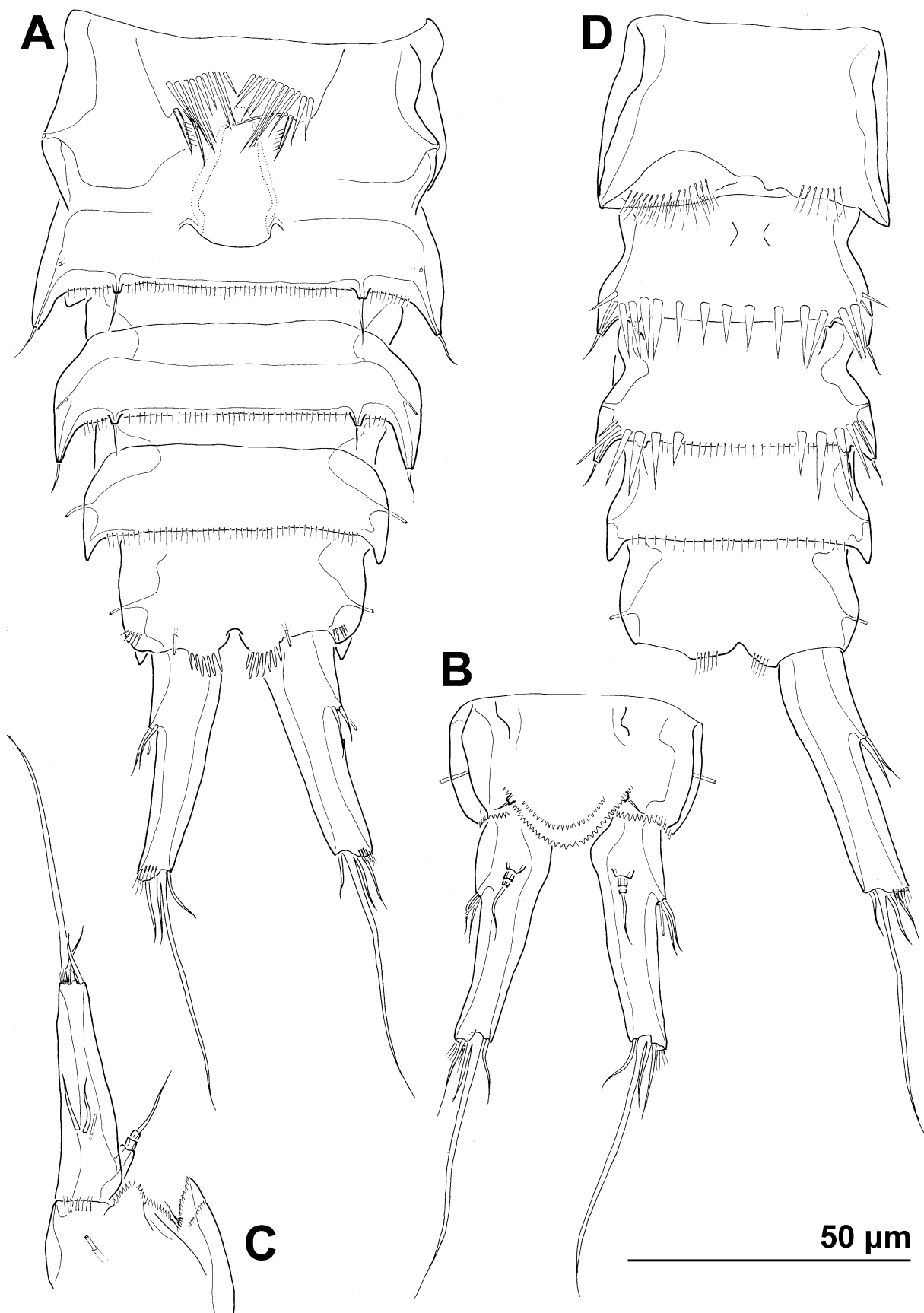
FIGURE 2. *Enhydrosoma apimelon* **sp. nov.**, SEM photographs, A-F, paratype ♀4; G, paratype ♀5; H, paratype ♀6: A, habitus, ventral; B, caudal rami, ventral; C, fifth leg, anterior; D, fifth leg, detail of endopodal peduncle, anterior; E, fifth leg, apical part of exopod, anterior; F, mouth appendages, ventral; G, anal somite and caudal rami, lateral; H, antenna and mouth appendages, ventral.
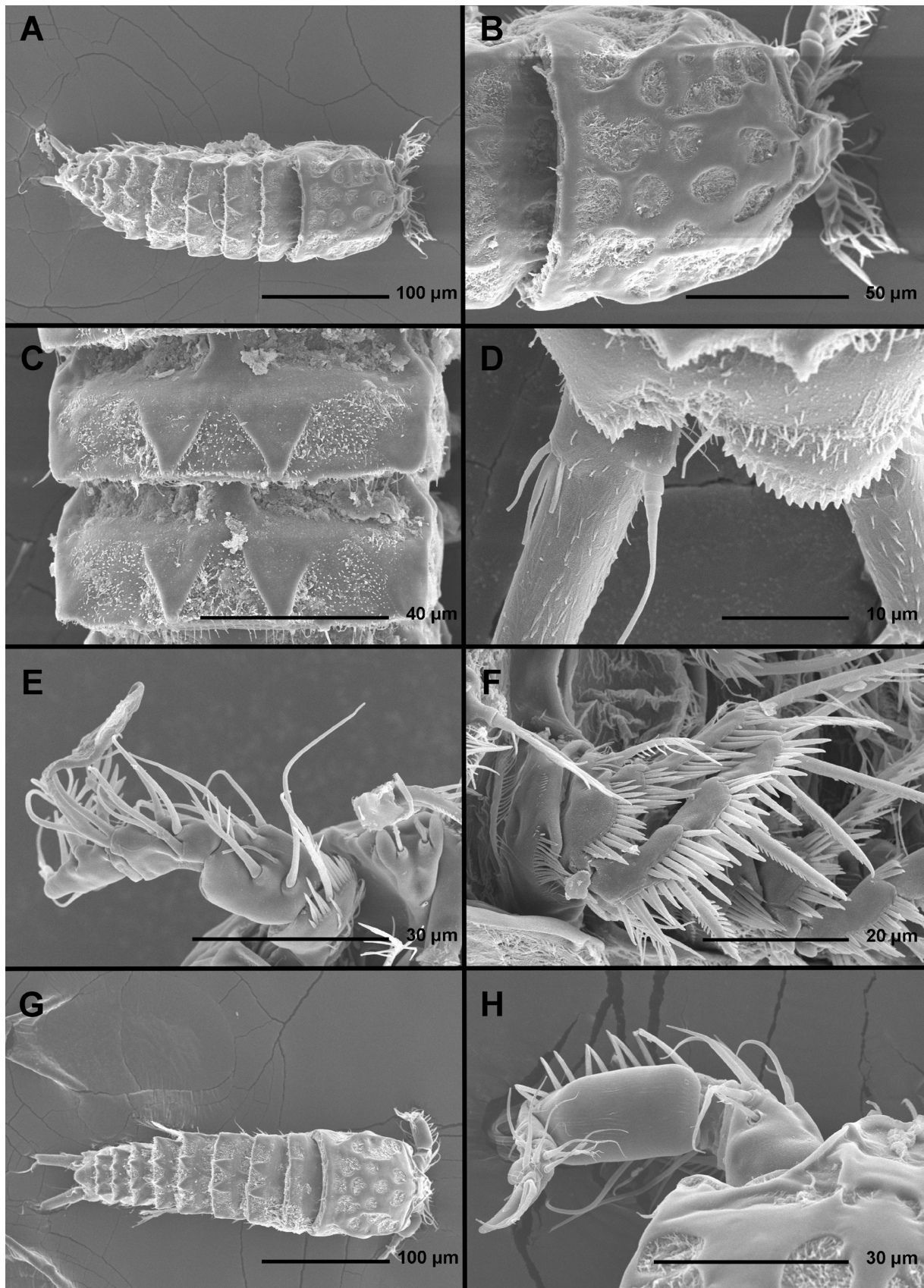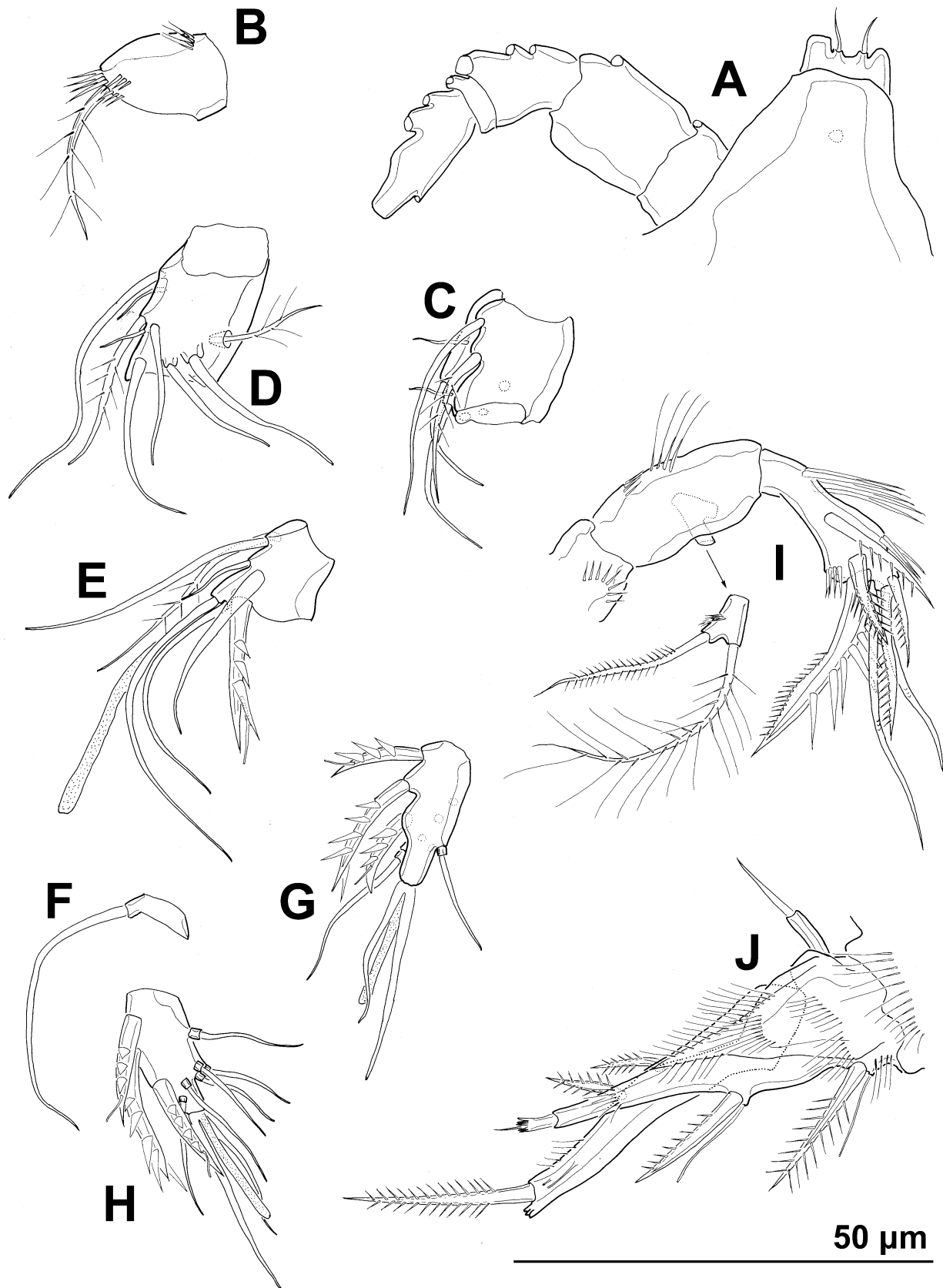
FIGURE 3. *Enhydrosoma apimelon* **sp. nov.**, SEM photographs, A & B, paratype ♀7; C & D, paratype ♀8; E & F, paratype ♀9; G & H, paratype ♂1: A, habitus, dorsal; B, cephalic shield, dorsal; C, tergites of third and fourth pedigerous somites, dorsal; D, anal operculum and anterior part of caudal rami, dorsal; E, rostrum and antennula, ventral; F, first swimming leg, anterior; G, habitus, dorsal. H, left antennula, dorsal.
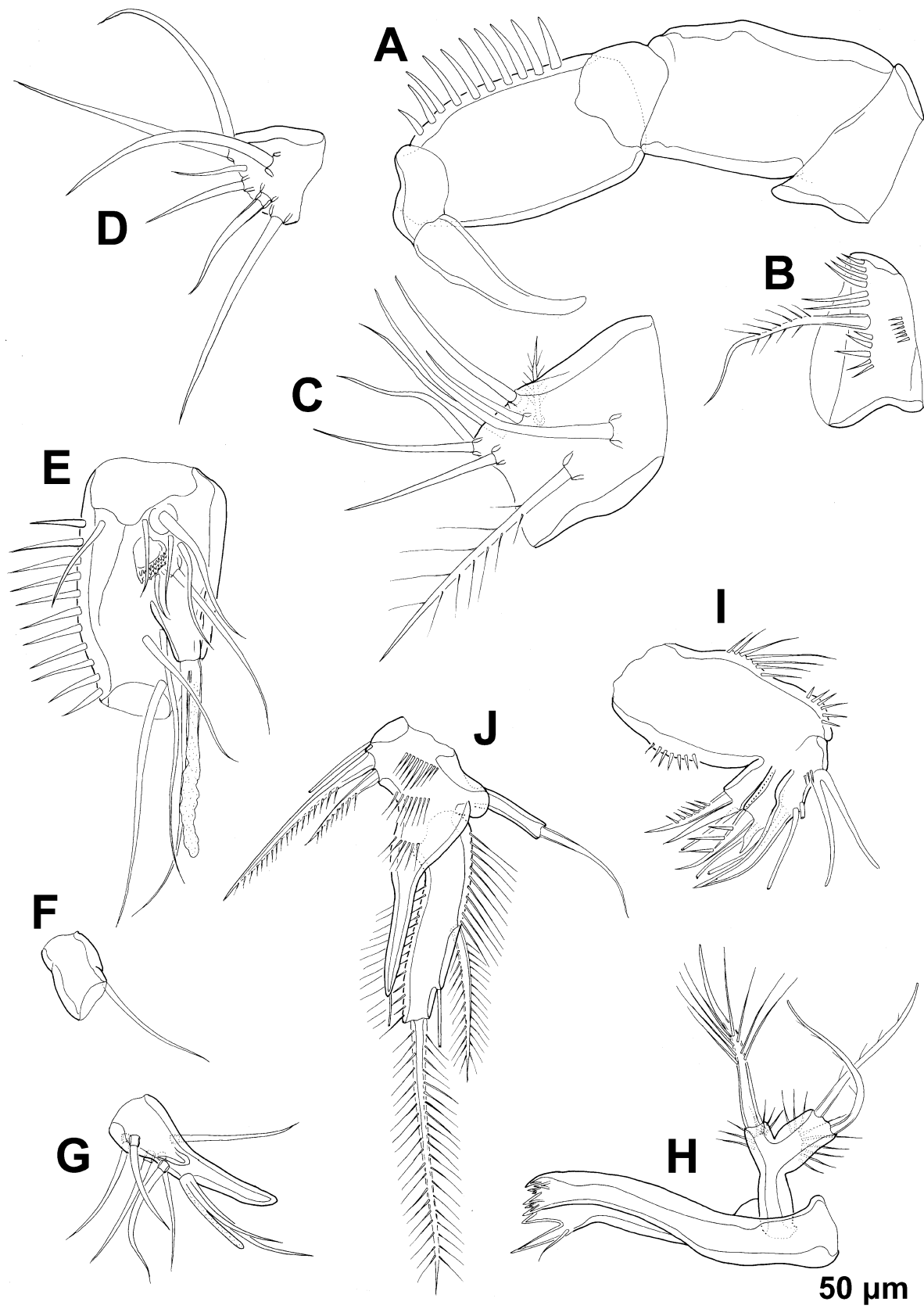
FIGURE 4. *Enhydrosoma apimelon* **sp. nov.**, SEM photographs, A-E, paratype ♂2; F & G, paratype ♂3; H, paratype ♂4: A, habitus, ventral; B, last two urosomites and caudal rami, ventral; C, fifth and sixth legs, anterior; D, right antennula, ventral. E, left antennula, ventral (distal part broken off); F, left antennula, ventral; G, rostrum, antero-ventral; H, antenna, ventral.

FIGURE 5. *Enhydrosoma apimelon* **sp. nov.**, line drawings, A-C, paratype ♀10; D, paratype ♂5: A, urosome, ventral; B, anal somite and caudal rami, dorsal; C, anal somite and right caudal ramus, lateral; D, urosome, ventral.
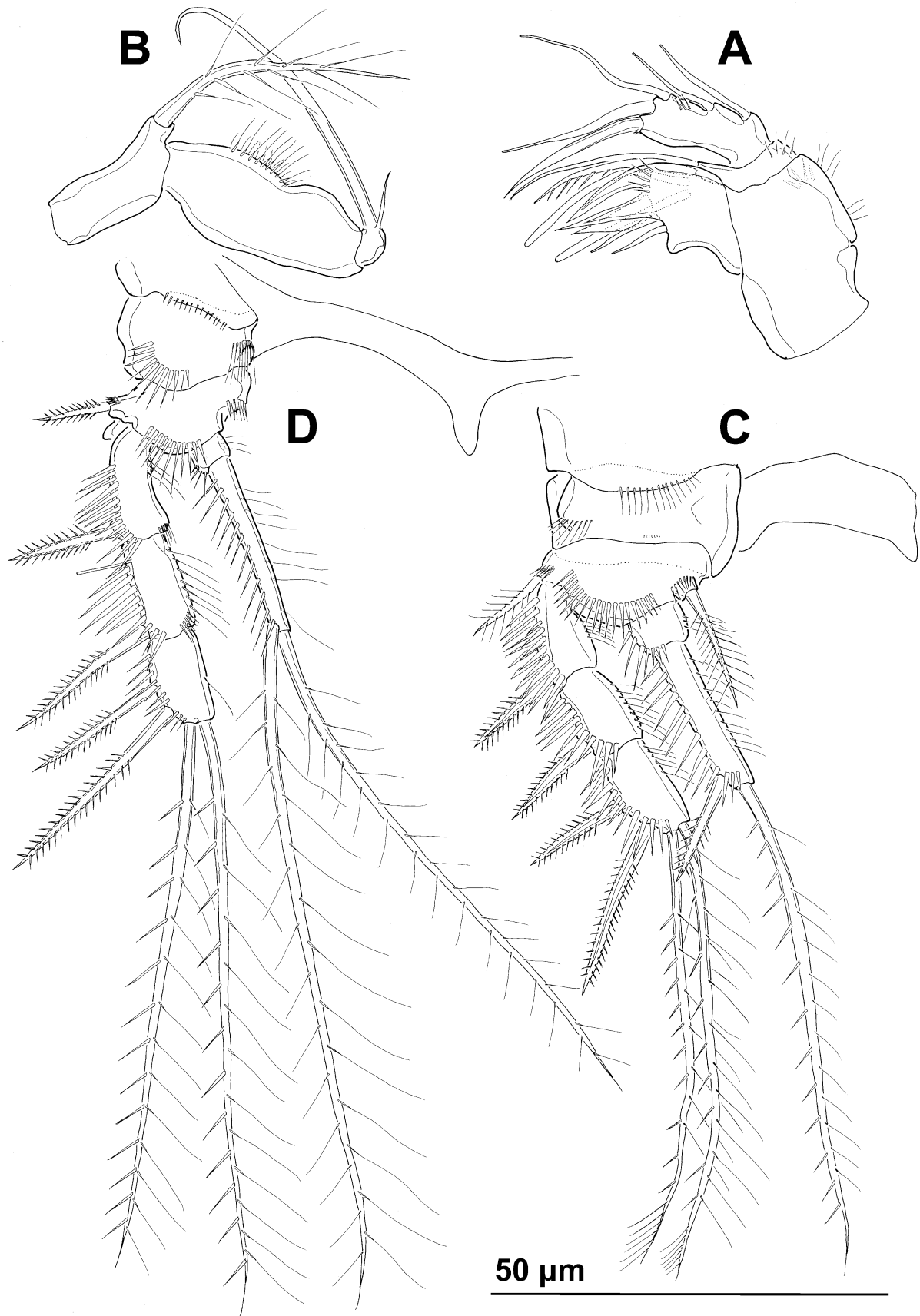
FIGURE 6. *Enhydrosoma apimelon* **sp. nov.**, line drawings, paratype ♀10: A, rostrum and left antennula without armature, dorsal; B, first segment of antennula, ventral; C, second segment of antennula, ventral; D, second segment of antennula, dorsal; E, third segment of antennula, dorsal; F, fourth segment of antennula, ventral; G, fifth segment of antennula, ventral; H, fifth segment of antennula, dorsal; I, antenna, posterior; J, fifth leg, anterior.
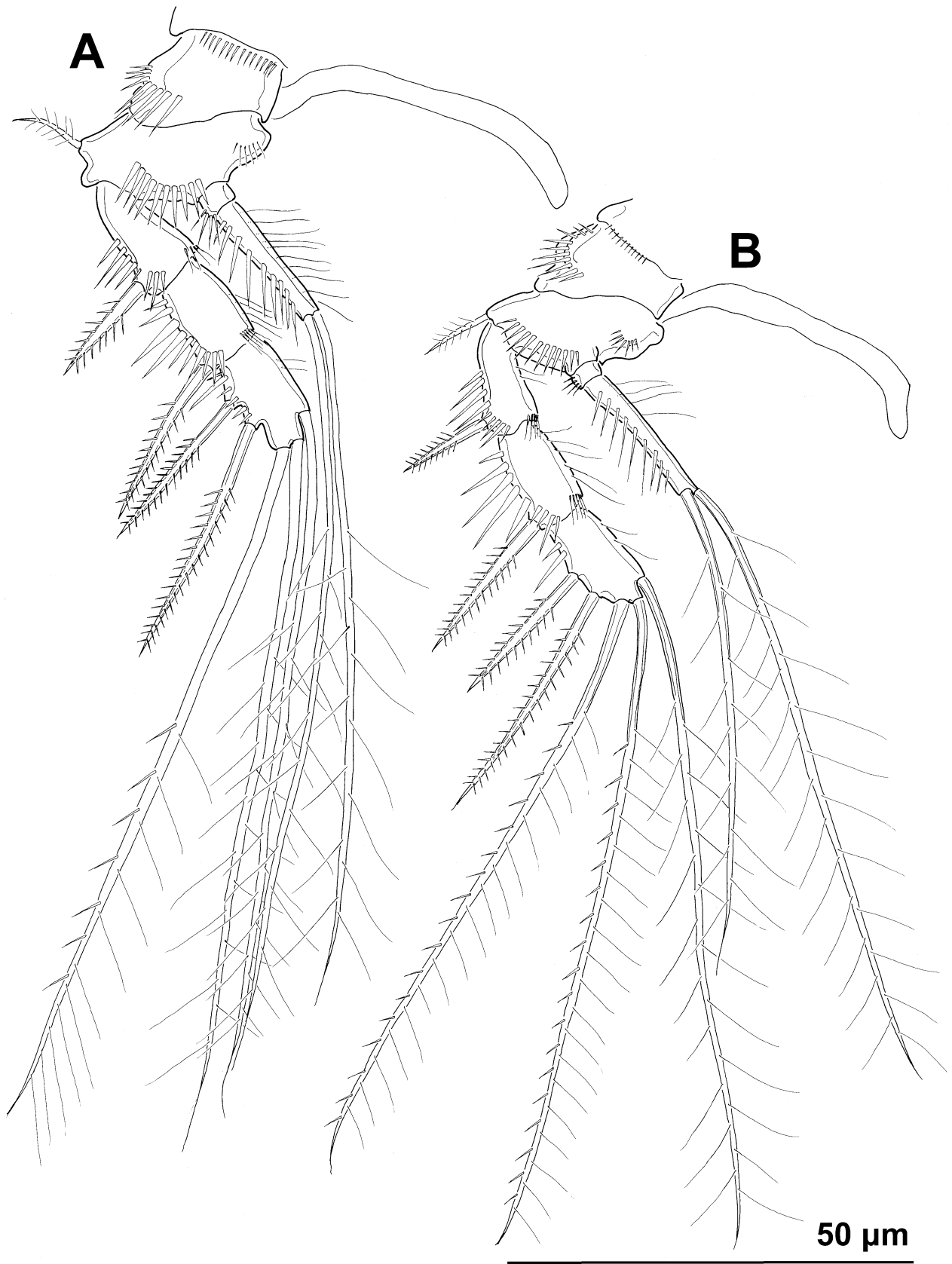
FIGURE 7. *Enhydrosoma apimelon* **sp. nov.**, line drawings, A-G & J, paratype ♂5; H & I, paratype ♀10: A, antennula without armature, ventral; B, first segment of antennula, ventral; C, second segment of antennula, ventral; D, third segment of antennula, ventral; E, fourth segment of antennula, ventral; F, fifth segment of antennula, ventral; G, sixth segment of antennula, ventral; H, mandible, posterior; I, maxilla, anterior; J, fifth leg, anterior.

FIGURE 8. *Enhydrosoma apimelon* **sp. nov.**, line drawings, paratype ♀10: A, maxillula, posterior; B, maxilliped, posterior; C, first swimming leg, anterior; D, second swimming leg, anterior.

FIGURE 9. *Enhydrosoma apimelon* **sp. nov.**, line drawings, paratype ♀10: A, third swimming leg, anterior; B, fourth swimming leg, anterior.

Fifth leg (Figs. 4C, 7J) somewhat smaller than in female but with similar basic structure; exopod with one lateral armature element, longer spinules, longer tubular pore, lacking distal frill. Endopodal spines inserted closer to each other, proximal spine significantly longer than distal spine; endopodal lobe without distal frill of fused spinules and without distal seta, with tubular pore on tip instead. Apical exopodal element about 1.3 times as long as proximal endopodal spine, 2.7 times as long as distal endopodal spine, 1.8 times as long as lateral exopodal element, and 1.3 times as long as exopod.

Sixth legs (Figs. 4C, 5D) simple cuticular plates, unarmed, with transverse row of slender, long spinules; left leg completely fused with somite, right leg transformed into functional genital operculum.

Variability. Despite numerous examined specimens and detailed examination using SEM, we are not able to report on any significant morphological variability.

Enhydrosoma robustum **sp. nov.**
(Figs. 10–15)

Type locality. South Korea, West Coast, Yellow Sea, Garorim Bay, muddy sediments, N 3658'32.3"N 12619'17.9"E.

Specimens examined. Holotype female (NIBRIV 0000287216) preserved in 70% ethanol collected from the type locality, 1 November 2012, collected by K. Kim. Dissected allotype male (NIBRIV 0000287217) mounted on one slide, collected from Korea, South Sea, Gwangyang Bay, sampling station 12 (see Karanovic *et al.* 2014), 34°53'24.50"N 127°47'42.40"E, 25 January 2006, collected by K. Kim. Additional paratypes: one female (NIBRIV 0000287218) preserved in 70% ethanol collected from the type locality; three dissected females (NIBRIV 0000287219, NIBRIV 0000287220, NIBRIV 0000287221) mounted on one slide each, collected from the type locality by K. Kim, 1 November 2012; one male and four females together on one SEM stub (NIBRIV 0000287222), collected from the type locality by K. Kim, 1 November 2012; three males and three females together on another SEM stub (NIBRIV 0000287223) collected from Korea, South Sea, Gwangyang Bay, sampling station 12 (see Karanovic *et al.* 2014), 34°53'24.50"N 127°47'42.40"E, 25 January 2006, collected by K. Kim. One female used for molecular analysis collected by K. Kim from the type locality on 1 November 2012 (see Table 1).

Etymology. The species name derives from the Latin adjective *robustus,* meaning "hard and strong like oak", and refers to the robust shape of the caudal rami. It was treated as an adjective, agreeing in gender with the neuter generic name.

Description of female. Based on holotype and several paratypes. Total body length from 287 to 342 µm (mean = 318 µm, n = 12). Body segmentation, colour, nauplius eye, hyaline fringes, general integument thickness, and most somite ornamentation as in *Enhydrosoma apimelon* **sp. nov.** However, surface relief on most somites different, and angle between telescopic and non-telescopic part of pleurons on most free somites much sharper (compare Figs. 1A and 10A). Habitus (Figs. 10A, G, 11A, C, 12A, C, E) generally cylindrical in dorsal view, widest at posterior end of cephalothorax and tapering posteriorly, boundary between prosome and urosome inconspicuous; prosome/urosome length ratio about 1.4, and prosome only slightly more voluminous than urosome. Body length/ width ratio about 3.8 in dorsal view; cephalothorax about 1.4 times as wide as genital double-somite. Free pedigerous somites without lateral or dorsal expansions, heavily sculptured, pleurons only partly covering coxae of swimming legs in lateral view. Integumental relief more defined by depressions than ridges in dorsal and lateral view; ventro-lateral ridges on urosomites as in *E. apimelon*. Most cuticular depressions and posterior margin of somites without hair-like spinules (except ventrally on urosomites), but full of bacterial growth and detritus, hindering observation of cuticular pores and sensilla . Hyaline fringe of all somites narrow and rough, in some places nearly serrated. In addition to hair-like spinules, surface ornamentation of somites and caudal rami consists of at least two different types of sensilla (slender and bottle-shaped; see Fig. 10D, F), simple cuticular pores, tubular pores, and few stronger spinules; exact number of pores and spinules difficult to establish.

Rostrum (Figs. 10B, 11D, 13A) as in *E. apimelon,* except for space between sensilla smaller than one horn-like projection.

Cephalothorax (Figs. 10B, C, D, 11D, E) shape as in *E. apimelon*, but with completely different relief, without comb of long setules in anterior part along interior surface of lateral margin (Fig. 11D), instead ventral margin produced ventrally into two characteristic flaps that protect first three pairs of mouth appendages (Fig. 11E), and

distal part of lateral margin finely serrated (Fig. 10C). Dorsal surface depressions more elongated than in *E. apimelon* (compare Figs. 3B and 10G), and lateral depressions smaller (compare Figs. 1B and 10B), but most sensilla easy to homologize.

Pleuron of free prosomites (Figs. 10E, 12A) very similar to each other, lacking triangular dorsal plates, conical mound-looking protuberances at base of sensilla, and posterior hair-like spinules; with oval dorsal and semi-circular lateral depressions. H higher areas of relief not defined into ridges and surface less smooth; in addition to sensilla homologous to those in *E. apimelon*, each free prosomite with one anterior dorso-lateral pair of small pores, and one central dorsal pair of large pores.

First urosomite (Figs. 10A, G, 12A) slightly longer and narrower than fourth pedigerous somite and pleuron without free lateral margin, but relief very similar to that of other pedigerous somites.

Genital double-somite (Figs. 10G, 11A, F, 12A, C, E, 14A) 1.3 times as wide as long in ventral view; completely fused ventrally but with deep suture indicating original segmentation between genital and third urosomites dorsally, thus dividing double-somite into equally long and similarly wide halves; ventral surface relatively smooth and flat, with ornamentation as in *E. apimelon* and with ventro-lateral ridges pronounced and produced posteriorly with pore on tip (Fig. 14A). Dorsal and lateral surfaces with relief, but without pronounced ridges and posterior protrusions; female genital complex (Fig. 14A) weakly sclerotized and hardly distinguishable from internal sutures and soft tissue, except for large copulatory pore near midlength of somite and wide copulatory duct; genital operculum as in *E. apimelon*.

Third urosomite (Figs. 10G, 11A, F, 12A, C, E, 14A) very similar in shape and ornamentation to posterior part of genital double-somite, with flat ventral surface, large posterior projections of ventro-lateral ridges with sensilla on tip, pair of ventral posterior sensilla, posterior row of ventral and lateral hair-like spinules, ventro-lateral pores, and two posterior dorsal pairs of sensilla; no dorso-lateral ridges, with nearly semi-circular shape in cross-section.

Fourth urosomite (Figs. 10G, 11A, C, G, 12A, C, E, G, 14A) shorter and narrower than third urosomite, with shorter posterior projections of dorso-lateral and ventro-lateral ridges, without sensilla, ornamented with pair of ventro-lateral pores, and posterior row of long hair-like spinules on ventral and partly on lateral surface.

Anal somite (Figs. 10H, 11G, 12G, 14A, B) only slightly clefted medially, with one pair of large dorsal sensilla at base of anal operculum, one pair of dorso-lateral simple pores, one pair of lateral simple pores, and one pair of ventral simple pores; ventro-lateral corners produced as in preanal somite, but slightly shorter. Anal operculum (Figs. 10H, 14B) semi-circular, short, only reaching slightly beyond midlength of somite, serrated, representing 43% of somite's width; anal sinus (Figs. 10H, 14B) widely open, without hair-like spinules.

Caudal rami (Figs. 10H, 11B, G, 12B, G, 14A, B) long, stout, about twice as long as anal somite, widest in central part, with narrower base and only tapering posteriorly at distal quarter, about twice as long as wide (ventral view), slightly divergent, with strong dorsal ridge giving near triangular cross-section, with very small space between them. Anterior part of medial margin flat; armature as in *E. apimelon* but dorsal and anterior lateral setae inserted much more posteriorly (at about 3/5 of ramus' length). Ornamentation consisting of several hair-like spinules on ventral side posteriorly and at base of distal lateral seta, and small spinules along ridges; no tubular pore at base of anterior lateral setae; outer distal process carrying posterior lateral seta even more produced than in *E. apimelon*; proportion of setae similar to that in *E. apimelon*; principal apical seta 1.3 times as long as caudal rami.

Antennula (Figs. 11D, 12D, F, H, 13A, 14C) short, stout, and five-segmented, as in *E. apimelon*. Lengthof segments and most armature as in *E. apimelon,* except for second segment with only seven setae, thus armature formula: 1.7.7+ae.1.11+ae; as in *E. apimelon* one pinnate seta on third segment and all three pinnate setae on fifth segment recurved, spiniform, with very strong spinules only along convex surface.

Antenna (Figs. 11D, 12D, F, 15A), labrum (Fig. 11E), paragnaths (Fig. 11E), mandibula (Figs. 11E, 15B), maxillula (Fig. 11E), maxilla (Figs. 11E, 15C), maxilliped (Fig. 11E, H), first swimming leg (Fig. 15D, E), second swimming leg, third swimming leg (Fig. 15F), and fourth swimming leg (Fig. 15G) as in *E. apimelon,* except for small differences in proportion of certain segments and armature elements and very minor differences in ornamentation.

Maxilla (Fig. 15C) without tubular pore and inner row of spinules.

Endopod of third swimming leg (Fig. 15F) and especially endopod of fourth swimming leg (Fig. 15G) proportionately shorter than in *E. apimelon*, and all exopodal segments on all swimming legs also slightly shorter.
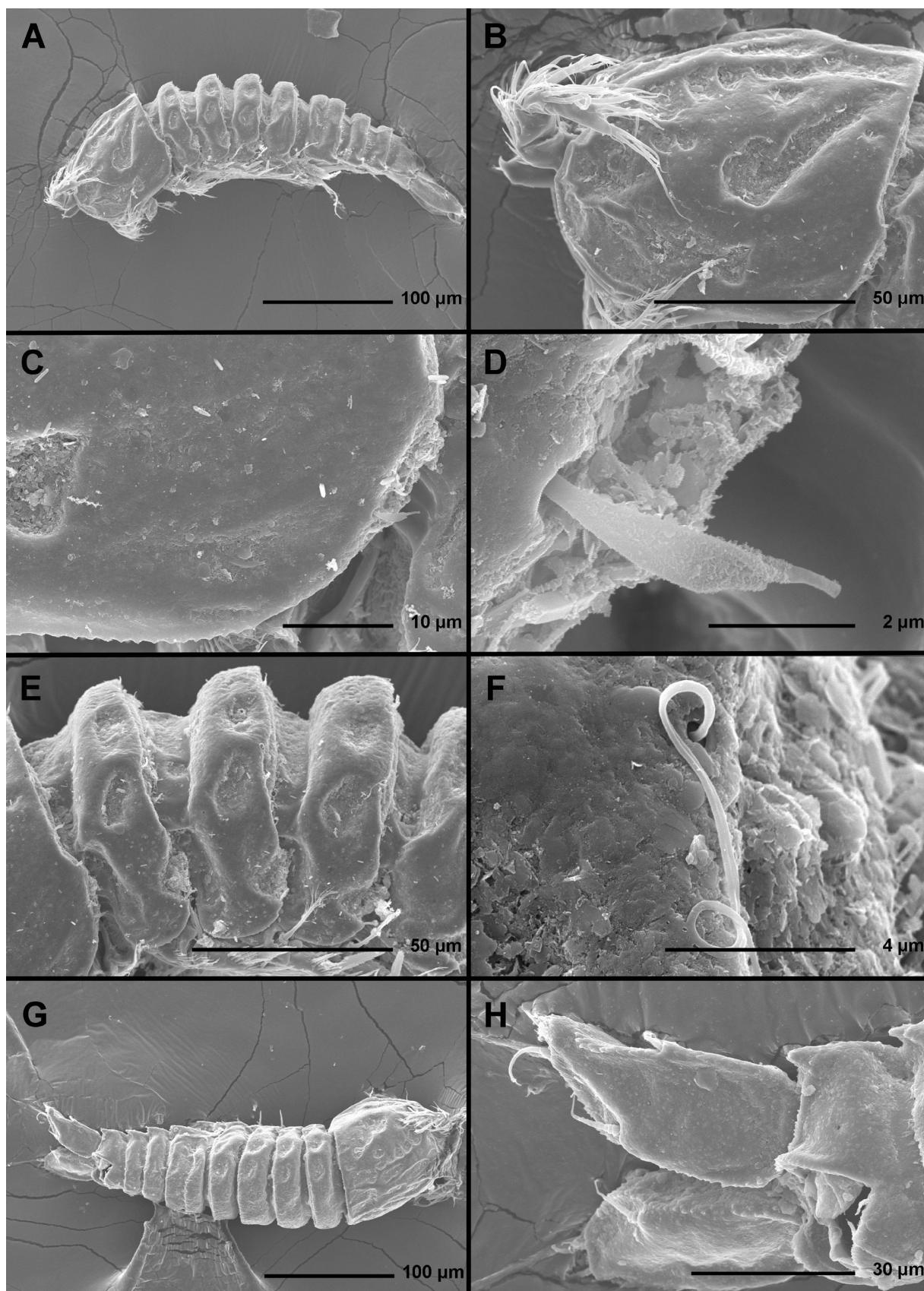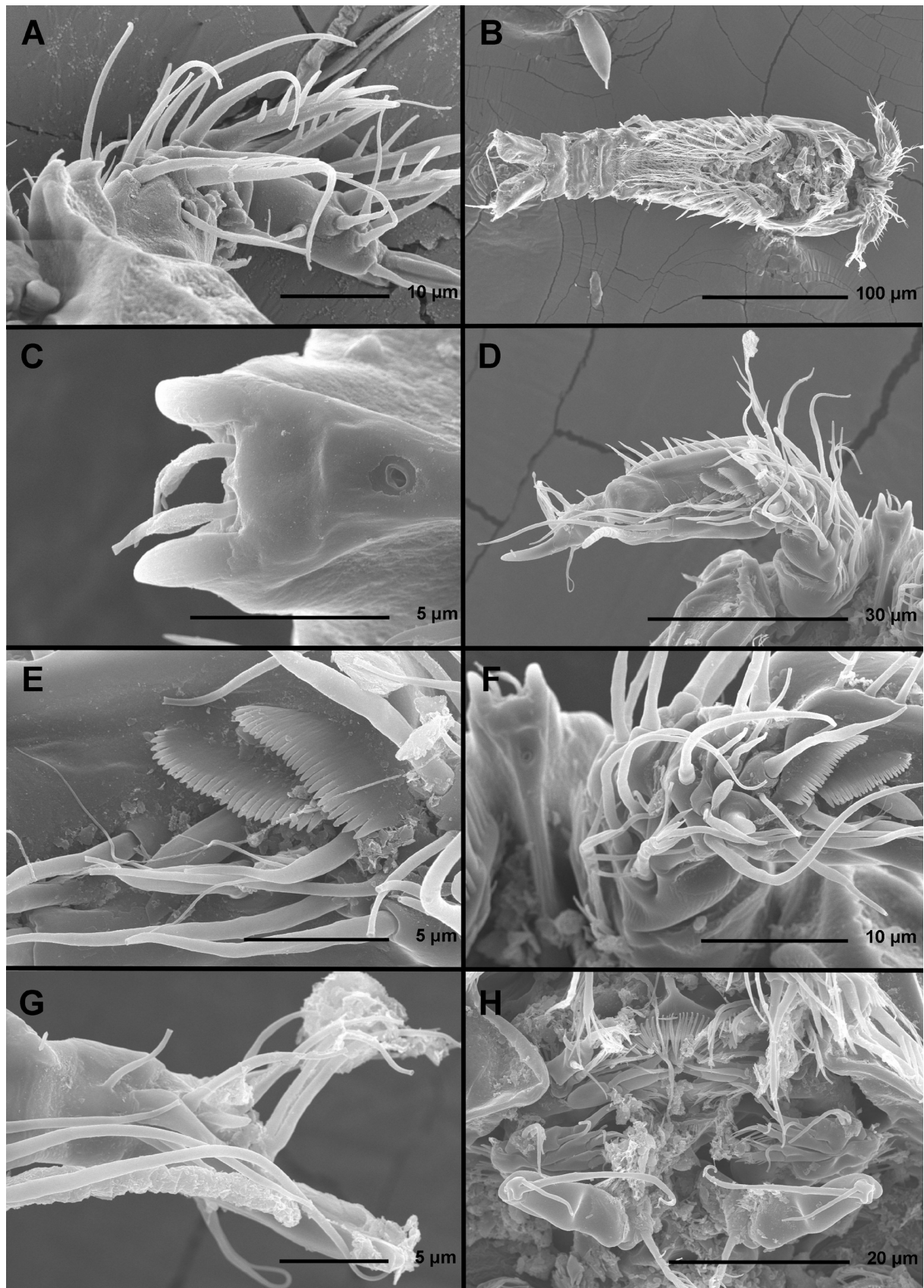
FIGURE 10. *Enhydrosoma robustum* **sp. nov.**, SEM photographs, A-F, paratype ♀1; G & H, paratype ♀2: A, habitus, lateral; B, cephalic shield, lateral; C, posterior-distal corner of cephalic shield, lateral; D, sensillum on posterior distal corner of cephalic shield; E, free prosomites, lateral; F, sensillum on central free prosomite; G, habitus, dorso-lateral; H, caudal rami, dorso-lateral.
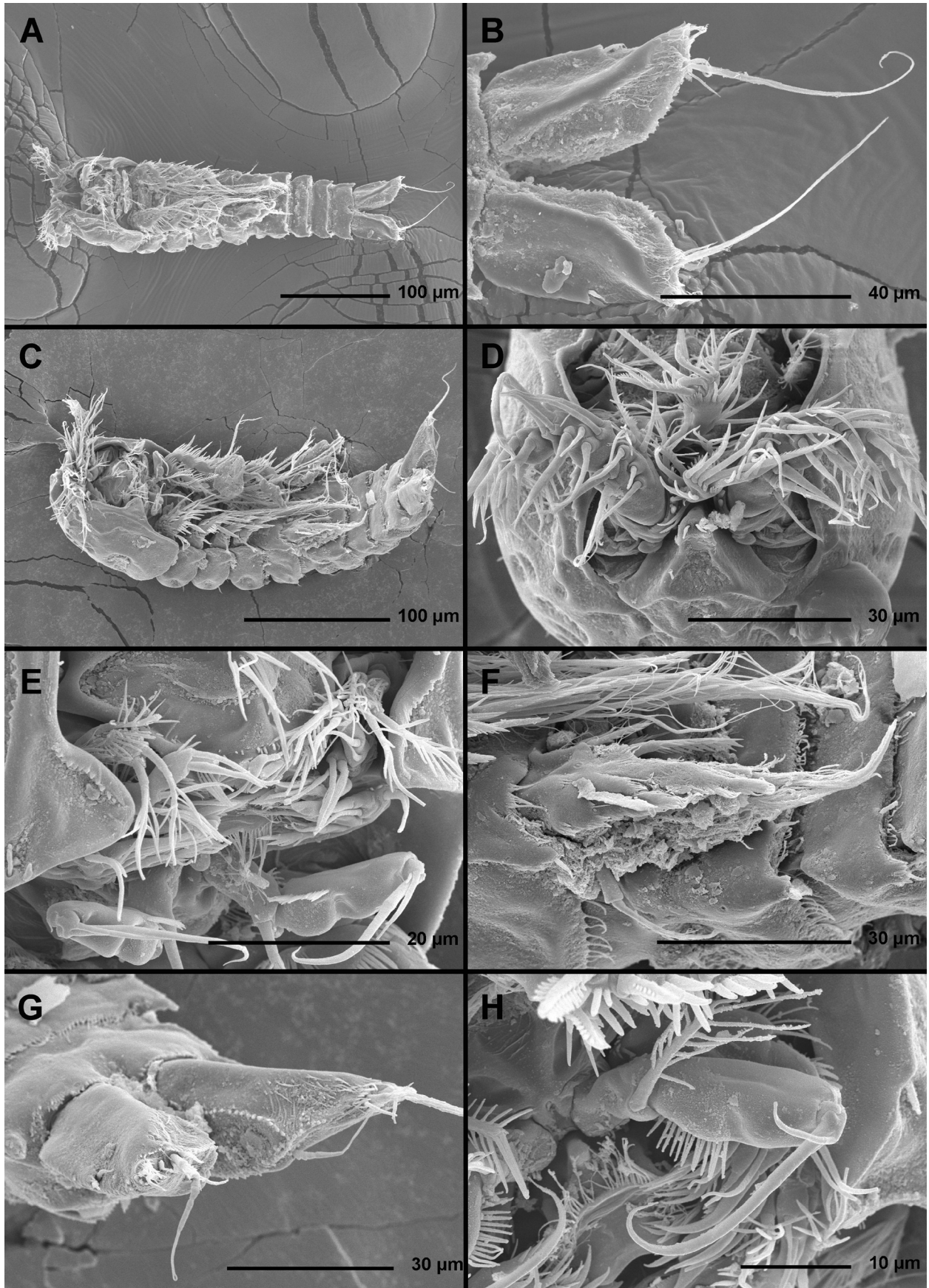
FIGURE 11. *Enhydrosoma robustum* **sp. nov.**, SEM photographs, A & B, paratype ♀3; C-G, paratype ♀4; H, paratype ♀5: A, habitus, ventral; B, caudal rami, ventral; C, habitus, ventral; D, rostrum, antennules, and antennae, ventral; E, mouth appendages, ventral; F, fifth leg, anterior; G, caudal rami, ventro-posterior; H, maxilliped, ventral.
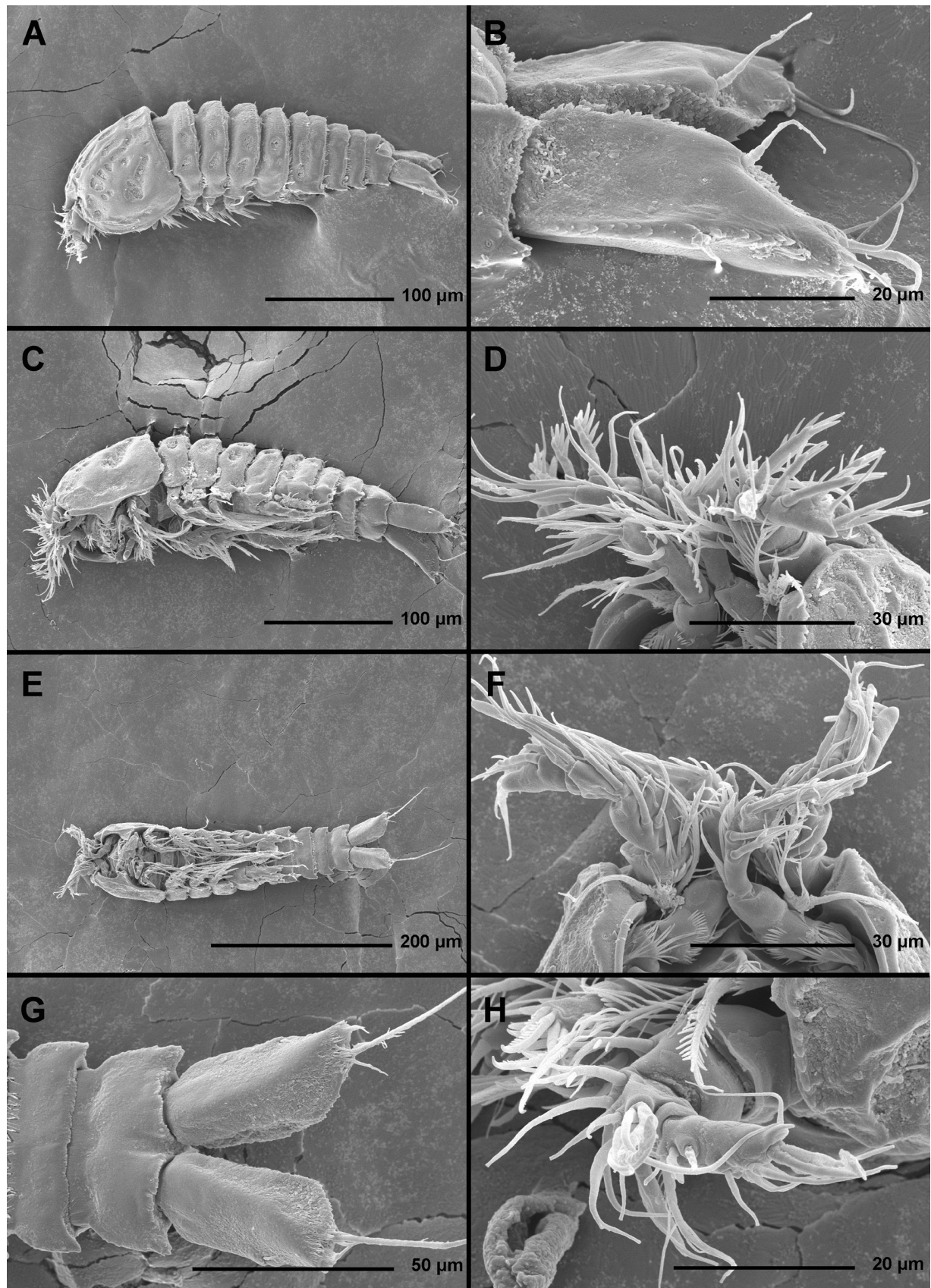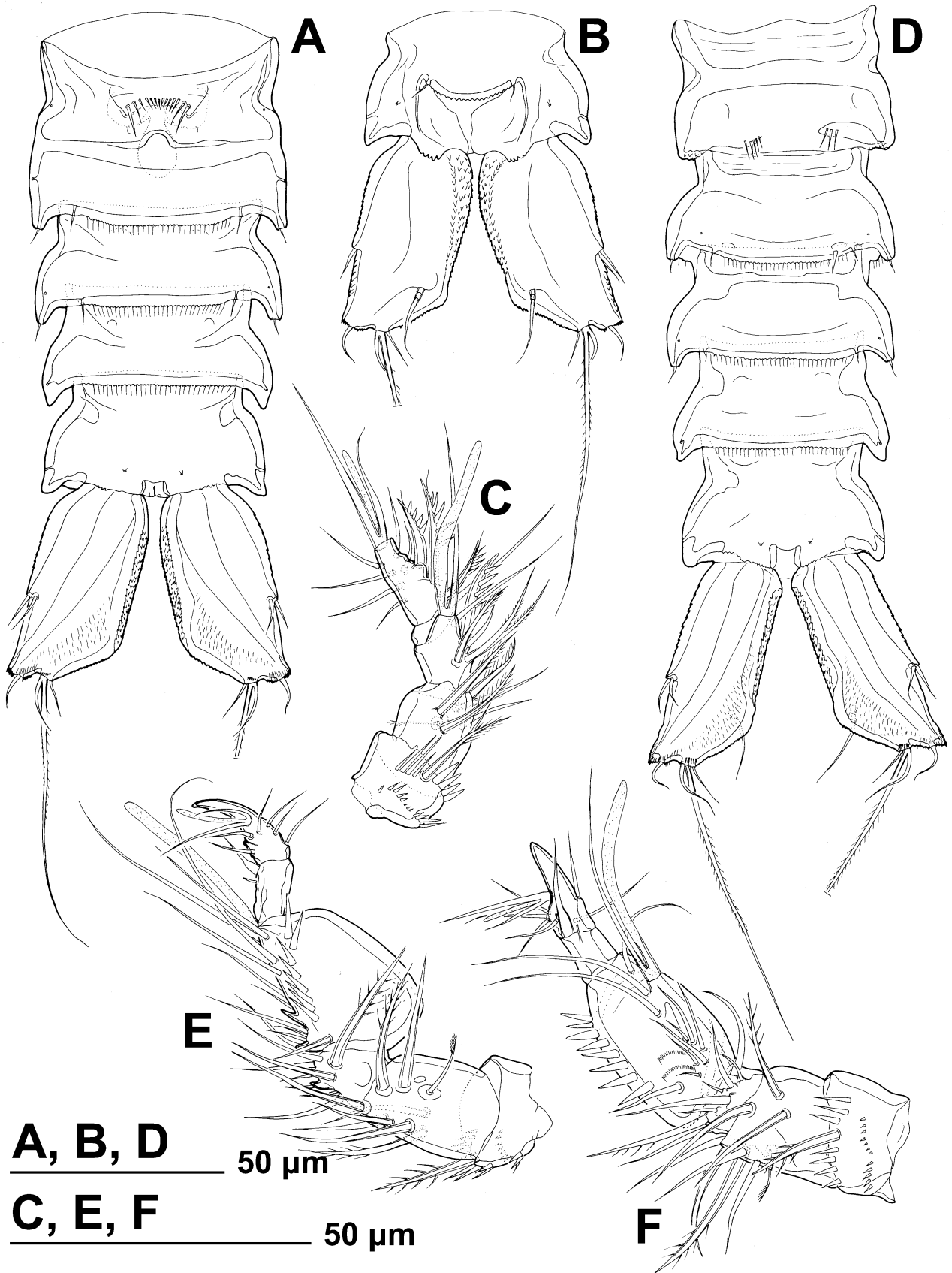
FIGURE 12. *Enhydrosoma robustum* **sp. nov.**, SEM photographs, A & B, paratype ♀6; C & D, paratype ♀7; E-G, paratype ♀8; H, paratype ♀9: A, habitus, lateral; B, caudal rami, lateral; C, habitus, ventro-lateral; D, antennulae and antennae, ventro-lateral; E, habitus, ventral; F, antennulae and antennae, ventral; G, last two urosomites and caudal rami, ventral; H, antennula, lateral.
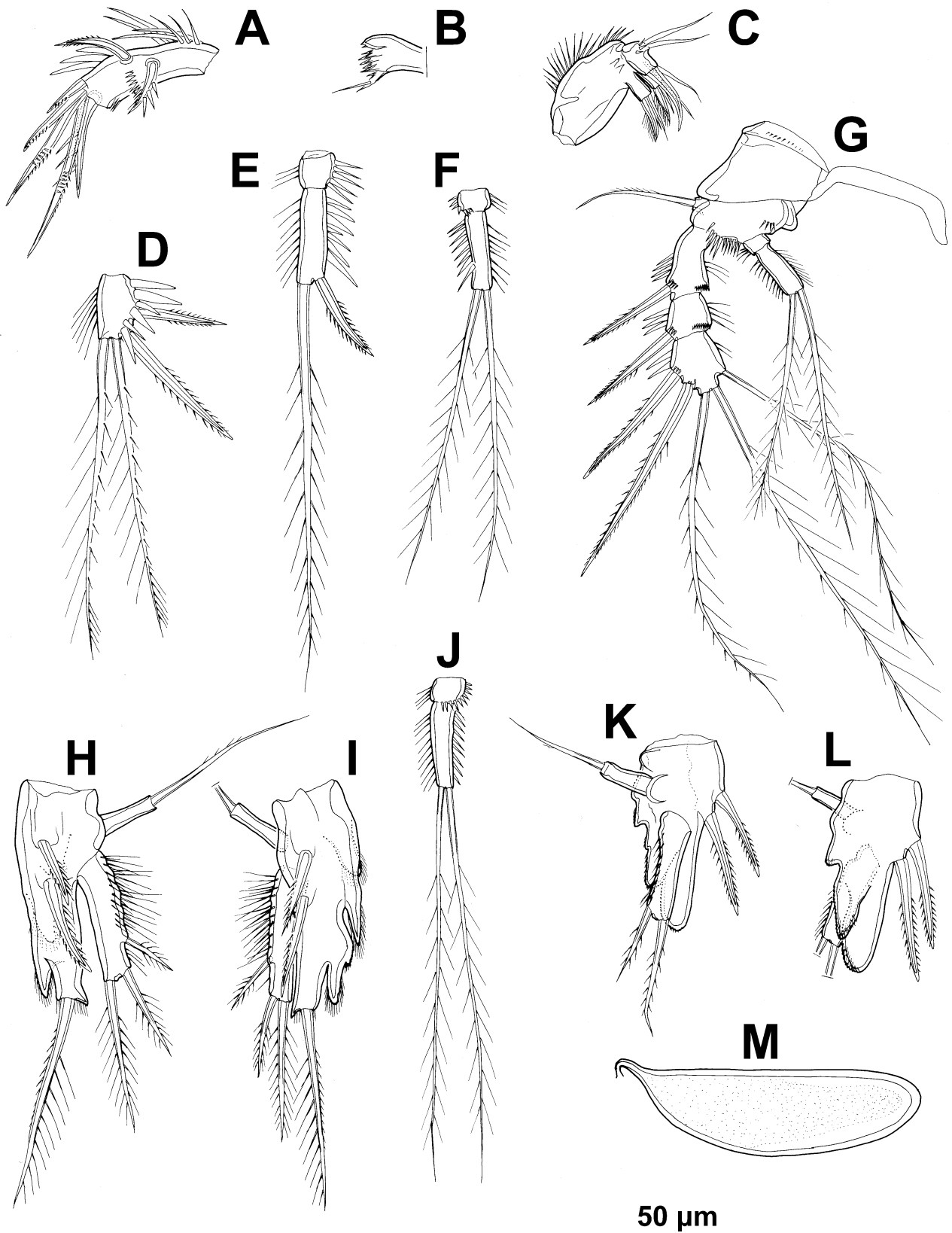
FIGURE 13. *Enhydrosoma robustum* **sp. nov.**, SEM photographs, A, paratype ♀10; B-H, paratype ♂1: A, rostrum and antennula, dorso-lateral; B, habitus, ventral; C, rostrum, ventral; D, right antennula, ventral; E, detail of right antennula, ventral; F, rostrum and proximal part of left antennula, ventral; G, distal part of left antennula, ventral; H, mouth appendages, ventral.

FIGURE 14. *Enhydrosoma robustum* **sp. nov.**, line drawings, A-C, paratype ♀11; D-F, allotype ♂: A, urosome, ventral; B, anal somite and caudal rami, dorsal; C, antennula, ventral; D, urosome, ventral; E, right antennula, dorsal; F, left antennula, ventral.

FIGURE 15. *Enhydrosoma robustum* **sp. nov.**, line drawings, A-I, paratype ♀11; J-M, allotype ♂: A, endopod of antenna, posterior; B, cutting edge of mandibula, anterior; C, maxilla, anterior; D, third exopodal segment of first leg, anterior; E, endopod of first leg, anterior; F, endopod of third leg, anterior; G, fourth leg, anterior; H, left fifth leg, antero-lateral; I, right fifth leg, anterior; J, endopod of third leg, anterior; K, left fifth leg, posterior; L, right fifth leg, anterior; M, spermatophore.

Fifth leg (Figs. 11F, 15H, I) biramous as in *E. apimelon*, comprising conical exopod and baseoendopod, but exopod slightly shorter than endopodal lobe; exopod also armed with three elements, but lateral elements inserted closer to distal margin than in *E. apimelon*, with distal lateral element almost subapical and difficult to homologize; outer margin of exopod with numerous long hair-like spinules, inner margin smooth. Baseoendopod armed with two inner strong spines and one distal seta as in *E. apimelon*, but distal seta much longer and very strong; inner margin of baseoendopod with three spiniform projections, each with tuft of hair-like spinules, and no tubular pores. Distal exopodal element about 2.2 times as long as proximal endopodal spine, 1.5 times as long as distal endopodal spine, 2.9 times as long as proximal exopodal element, 1.6 times as long as middle exopodal element, 0.7 times as long as distal endopodal element, and nearly 1.2 times as long as entire exopod.

Sixth legs (Fig. 14A) as in *E. apimelon*, but with relatively smaller basal spinules and outer element slightly longer than inner one.

Description of male. Based on allotype and four other paratypes. Body length from 279 to 312 µm (mean = 302 µm, n = 5). Genital somite and third urosomite not fused (Fig. 14D). Habitus (Fig. 13B), colour, rostrum (Fig. 13C), shape and ornamentation of cephalothorax and free prosomites (Fig. 13B), shape and ornamentation of last three urosomites (Figs. 13B, 14D), general shape, armature and ornamentation of caudal rami (Figs. 13B, 14D), antenna (Fig. 13B), labrum (Fig. 13H), paragnaths (Fig. 13H), mandibula (Fig. 13H), maxillula (Fig. 13H), maxilla (Fig. 13H), maxilliped (Fig. 13H), and all swimming leg (Figs. 13B, 15J) as in female. Prosome/urosome ratio about 1.1, greatest width at posterior end of cephalothorax, body length/width ratio about 3.5; cephalothorax 1.6 times as wide as genital somite in dorsal view.

Genital somite (Fig. 14D) 1.5 times as wide as long in ventral view, as in *E. apimelon*, but with more pronounced central internal ridge and fewer spinules at base of reduced sixth legs; single large spermatophore (Fig. 15M) visible inside genital somite, about 3.2 times as long as wide without its neck.

Third urosomite (Figs. 13B, 14D) as posterior part of genital double-somite in female but proportionately narrower, and with one or two large ventro-lateral spinules.

Caudal rami (Figs. 13B, 14D) very similar to those in female but longer in proportion to anal somite and generally more elongated.

Antennula (Figs. 13D, E, F, G, 14E, F) as in *E. apimelon*, except fourth segment with two delicate parallel combs (Fig. 13E) instead of brush, additional small seta (or tubular pore?) present on fifth segment (Fig. 13G) and long apical seta on that segment swollen at base, fourth segment slightly larger.

Fifth leg (Fig. 15K, L) somewhat smaller than in female but with similar basic structure; exopod without proximal lateral armature element and with shorter spinules. Endopodal lobe without distal armature element, with relatively larger inner spines, and with smaller spinules on its three spiniform processes; endopodal inner spines of similar length and width.

Sixth legs (Fig. 14D) as in *E. apimelon*, simple cuticular plates, unarmed, with transverse row of several slender spinules.

Variability. Despite numerous examined specimens and detailed examination using SEM (see Figs. 10A, G, 11A, C, 12A, C, E, 13B), we are not able to report on any significant intraspecific morphological variability. The number of ventro-lateral spinules on the third urosomite in male varies between zero and three.

Enhydrosoma kosmetron **sp. nov.**
(Figs. 16–21)

Type locality. South Korea, South Sea, Gwangyang Bay, sampling station 3 (see Karanovic *et al.* 2014), muddy sediments, 3453'03.9"N 12739'50.5"E.

Specimens examined. Holotype female (NIBRIV 0000287224) dissected and mounted on one slide, collected from the type locality, 17 February 2013, collected by K. Kim. Allotype male (NIBRIV 0000287225) dissected and mounted on one slide, collected from Korea, South Sea, Gwangyang Bay, sampling station 10 (see Karanovic *et al.* 2014), 34°55'15.4"N 127°47'07.9"E, 18 February 2012, collected by K. Kim. Additional paratypes: one dissected female (NIBRIV 0000287226) mounted on one slide; four males and two females together on one SEM stub (NIBRIV 0000287227); three males and three females together on another SEM stub (NIBRIV 0000287228); all from Korea, South Sea, Gwangyang Bay, sampling station 10 (see Karanovic *et al.* 2014), 34°55'15.4"N 127°47'07.9"E, 18 February 2012, collected by K. Kim. One female used for molecular analysis collected by K. Kim from the type locality on 26 July 2012 (see Table 1).

Etymology. This species is named after the Greek noun *kosmetron,* meaning "broom" and referring to the broom-like ornamentation of the male antennulae. The specific name is to be treated as a noun (gender masculine) in apposition to the generic name.

Description of female. Based on holotype and several paratypes. Total body length from 441 to 495 μm (mean = 483 μm, n = 7). Body segmentation, colour, nauplius eye, hyaline fringes, general integument thickness, angle between telescoped and non-telescoped parts of pleurons on most free somites, and most somite ornamentation as in *Enhydrosoma apimelon* **sp. nov.**, however, surface relief on most somites slightly different. Habitus (Figs. 16A) generally cylindrical in dorsal view, widest at posterior end of cephalothorax and tapering posteriorly, boundary between prosome and urosome inconspicuous; prosome/urosome length ratio about 1.1, and prosome only slightly more voluminous than urosome. Body length/width ratio about 3.7 in dorsal view; cephalothorax about 1.2 times as wide as genital double-somite. Free pedigerous somites without lateral or dorsal expansions, heavily sculptured, pleurons only partly covering coxae of swimming legs in lateral view. Integumental relief more defined by ridges than depressions in dorsal and lateral view; ventro-lateral ridges on urosomites as in *E. apimelon*, but ventral surface with additional (mostly internal) ridges. Most cuticular depressions and posterior margin of prosomites without hair-like spinules but full of bacterial growth and detritus, making observation of cuticular pores and sensilla in those regions very difficult; posterior margin of urosomites with hair-like spinules, especially on ventral surface. Hyaline fringe of all somites narrow and rough, in some places nearly serrated, and in all but last two somites also with conical mound-looking protuberances with sensilla on tip, as in *E. apimelon*. In addition to hair-like spinules, surface ornamentation of somites and caudal rami consists of at least two different types of sensilla (slender and bottle-shaped; see Fig. 16C), simple cuticular pores, and few stronger spinules; exact number of pores and spinules difficult to establish.

Rostrum (Fig. 16B, E) as in *E. apimelon,* except for space between sensilla smaller than width of one horn-like projection.

Cephalothorax (Fig. 16B) as in *E. apimelon*, but with completely different relief in dorsal view, without oval depression and with more pronounced longitudinal ridges (compare Figs. 3B and 16B), without comb of long setules in anterior part along inner surface of lateral margin (as observed in *E. apimelon*) or ventral flaps that protect first three pairs of mouth appendages (as observed in *E. robustum* **sp. nov.**); lateral relief similar to that in *E. apimelon*, except for posterior depression larger and more triangular; most sensilla easy to homologize.

Pleuron of free prosomites (Fig. 16A) very similar to each other, without triangular dorsal plates and posterior hair-like spinules, but with posterior conical mound-looking protuberances at base of sensilla, as well as dorsal and dorso-lateral ridges similar to those in *E. apimelon* but slightly smaller; all sensilla homologous to those in *E. apimelon*; angle between telescoped and non-telescoped parts of pleuron relatively wide as in *E. apimelon*.

First urosomite (Fig. 16A) slightly narrower and significantly longer than fourth pedigerous somite and pleuron without free lateral margin, but relief very similar to that of other pedigerous somites, with pronounced dorso-lateral ridges resulting in angular shape in cross-section.

Genital double-somite (Figs. 16A, 19A) 1.6 times as wide as long in ventral view; completely fused ventrally but with deep suture indicating original segmentation between genital and third urosomites dorsally, thus dividing double-somite into equally long and similarly wide halves; general shape and ornamentation as in *E. apimelon*, except for more pronounced ridges on ventral surface and additional pair of ventral pores. Female genital complex (Fig. 19A) weakly sclerotized and hardly distinguishable from internal sutures and soft tissue, except for large copulatory pore near midlength of somite and wide copulatory duct; genital operculum as in *E. apimelon* but with longer armature elements and shorter spinules.

Third urosomite (Figs. 16A, 19A) very similar in shape and ornamentation to posterior part of genital double-somite, but without ventral pores and with three or four large spinules on ventral surface at base of each ventral sensillum.

Fourth urosomite (Figs. 16A, D, 19A) slightly shorter and narrower than third urosomite and without any sensilla and large spinules, but with well-developed dorsal, dorso-lateral, and ventro-lateral ridges (latter finely serrated), with posterior row of hair-like spinules, and with ventro-lateral cuticular pores.

Anal somite (Figs. 16A, D, 19A, B) only slightly clefted medially, with one pair of large dorsal sensilla at base of anal operculum, several minute spinules, small group of large ventral spinules on medial corners, and one pair of ventral simple pores; ventro-lateral corners produced as in preanal somite, but slightly longer and more flared out, also serrated; dorso-lateral corner also produced into small serrated flaps; anal operculum (Figs. 16D, 19B) semi-

circular, short, not reaching posterior margin of somite (shorter than in *E. apimelon* but longer than in *E. robustum*), serrated, representing 39% of somite's width; anal sinus widely open, with three rows of hair-like spinules.

Caudal rami (Figs. 16A, D, 19A, B) spindle-shaped, widest at about proximal quarter of their length, about 1.4 times as long as anal somite, about 2.2 times as long as wide (ventral view), strongly divergent, with strong dorsal ridge, and with space between them about one ramus' width. Armature as in *E. apimelon* but dorsal seta longer and inserted more posteriorly (at about midlength); ornamentation as in *E. robustum*; no tubular pore at base of anterior lateral setae; outer distal process carrying posterior lateral seta even more produced than in *E. robustum*; proportion of setae other than dorsal similar to that in *E. apimelon*; principal apical seta 1.3 times as long as ramus.

Antennula (Figs. 16F, 20A) as in *E. apimelon*, except for second segment with one seta less (thus armature formula being: 1.8.7+ae.1.11+ae), and five additional spiniform setae and with strong spinules (three setae on second segment, one on third segment, and stronger apical seta on fifth segment). Lnegth and ornamentation of segments as in *E. apimelon*; as in *E. apimelon* and *E. robustum* one unipinnate slender seta on second segment inserted into cone-shaped depression.

Antenna (Figs. 19C), labrum, paragnaths, general shape and armature of maxilla (Fig. 20B), maxilliped (Fig. 20C), endopod of first swimming leg (Fig. 20D), second swimming leg (Fig. 20F), exopod of third swimming leg, and exopod of fourth swimming leg as in *E. apimelon* and *E. robustum,* except for small differences in proportion of certain segments and armature elements and very minor differences in ornamentation.

Mandibula (Fig. 19D) size and segmentation as in *E. apimelon*, but palp with four setae and seta on cutting edge of coxal gnathobase much stronger and longer.

Maxillula (Fig. 19E) size and segmentation as in *E. apimelon*, but both basis and praecoxal arthrite with one additional inner seta.

Maxilliped (Fig. 19C) as in *E. apimelon*, except endopodal strong spine shorter and slender endopodal seta proportionately longer; coxa ornamented with three rows of spinules.

Exopod of first swimming leg (Fig. 20E) with five elements on third segment.

Endopod of third swimming leg (Fig. 20G) and endopod of fourth swimming leg (Fig. 20H) both with very short outer spines in addition to two slender and long terminal setae on second segment.

Fifth leg (Fig. 20I) biramous as in *E. apimelon*, comprising conical exopod and baseoendopod, but exopod much more robust and endopodal lobe shorter; exopod also armed with three elements, but lateral elements inserted closer to distal margin (as in *E. robustum*), with distal lateral element almost apical and difficult to homologize, and apical element very small and bare. Outer margin of exopod with numerous long hair-like spinules, inner margin smooth, without tubular pores; baseoendopod as in *E. robustum* with robust distal seta, but with only one cuticular spiniform process on inner margin covered by small spinules; distal exopodal element about 0.3 times as long as proximal endopodal spine, 0.2 times as long as distal endopodal spine, 0.75 times as long as proximal exopodal element, 0.25 times as long as middle exopodal element, 0.3 times as long as distal endopodal element, and less than 0.2 times as long as entire exopod; exopod about 3.3 times as long as wide. Endopodal lobe without tubular pores, but with two simple pores at base of inner spines.

Sixth legs (Fig. 19A) as in *E. apimelon*, but with proportionately smaller basal spinules and larger armature; inner smooth seta about 1.7 times as long as outer unipinnate spine.

Description of male. Based on allotype and four other paratypes. Body length ranging from 279 to 312 μm (mean = 302 μm, n = 5). Genital somite and third urosomite not fused (Fig. 19F). Habitus (Figs. 16G, 17A, 18A), colour, rostrum, shape and ornamentation of cephalothorax (Fig. 18B, C, D), shape and ornamentation of free prosomites (Fig. 16G, 18A), shape and ornamentation of last three urosomites (Figs. 16H, 17C, H, 18H, 19F), general shape, armature and ornamentation of caudal rami (Figs. 16H, 17C, 18H, 19F), antenna (Fig. 17E), labrum (Fig. 17F), paragnaths (Fig. 17F), mandibula (Figs. 17F, 21C, D), maxillula (Fig. 17F, 21E), maxilla (Fig. 17B, F), maxilliped (Fig. 17F), first swimming leg (Fig. 17G), second swimming leg (Fig. 17A), exopod of third swimming leg (Fig. 17A), and fourth swimming leg (Fig. 21G) as in female. Prosome/urosome ratio about 1.2, greatest width at posterior end of cephalothorax, body length/width ratio about 3.3; cephalothorax 1.6 times as wide as genital somite in dorsal view.

Genital somite (Figs. 17H, 19F) 1.8 times as wide as long in ventral view, similar in ornamentation to that in *E. robustum*, and also with left sixth leg functioning as genital operculum; no spermatophore visible inside any observed specimens.
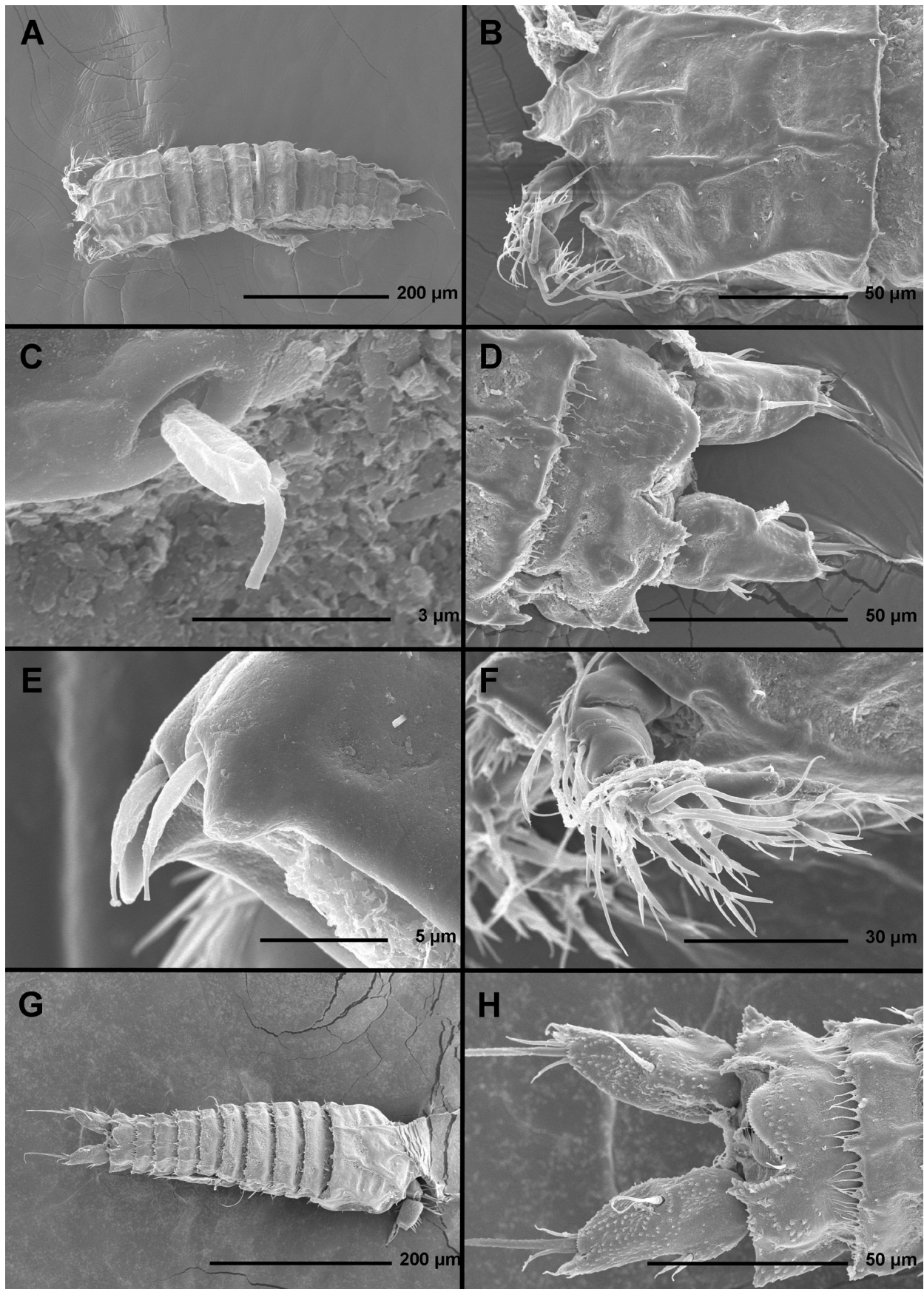
FIGURE 16. *Enhydrosoma kosmetron* **sp. nov.**, SEM photographs, A-D, paratype ♀1; E & F, paratype ♀2; G & H, paratype ♂1: A, habitus, dorsal; B, cephalic shield, dorsal; C, sensillum in central part of cephalic shield; D, anal somite and caudal rami, dorsal; E, rostrum, lateral; F, rostrum and left antennula, lateral; G, habitus, dorsal; H, anal somite and caudal rami, dorsal.
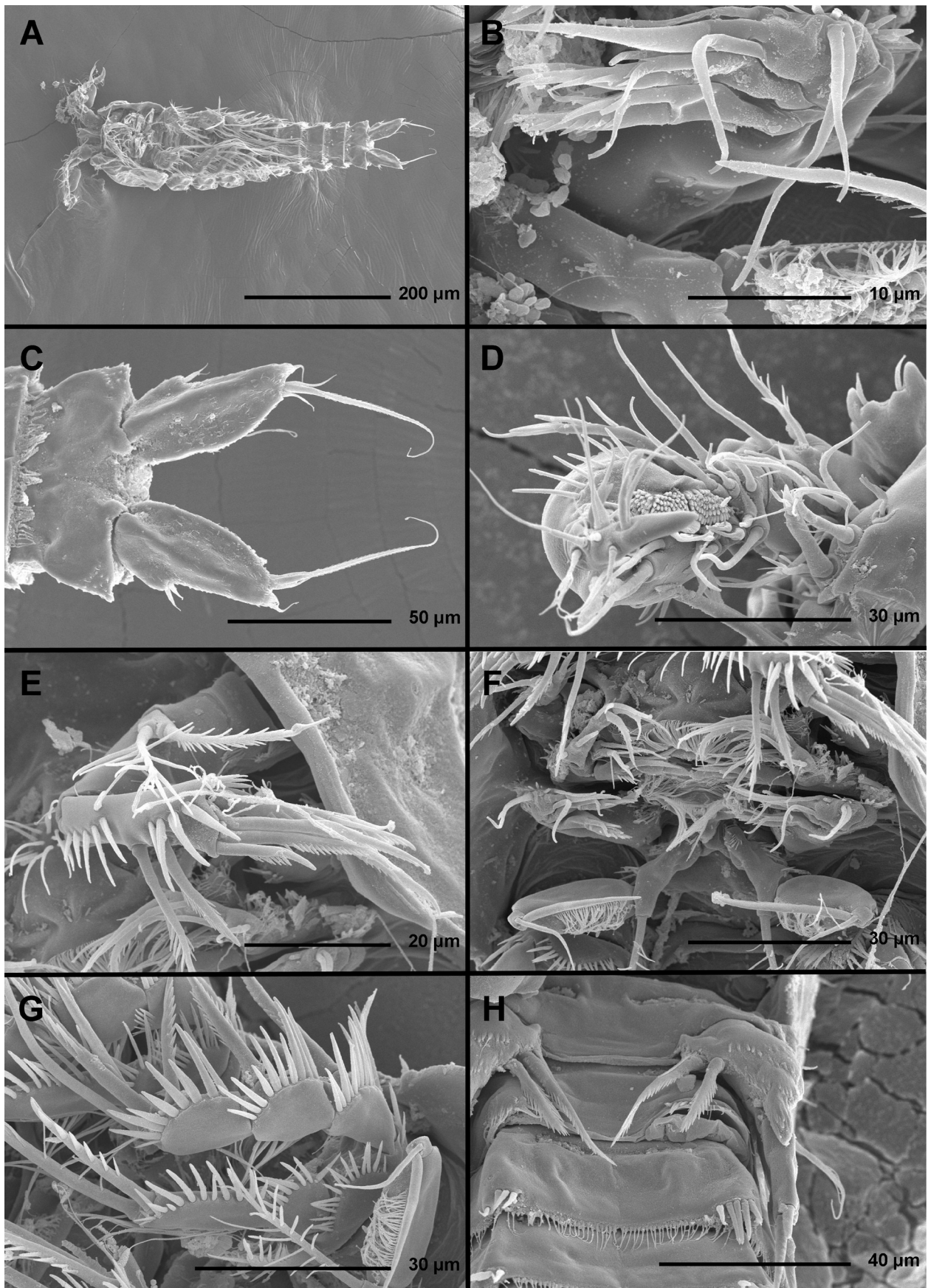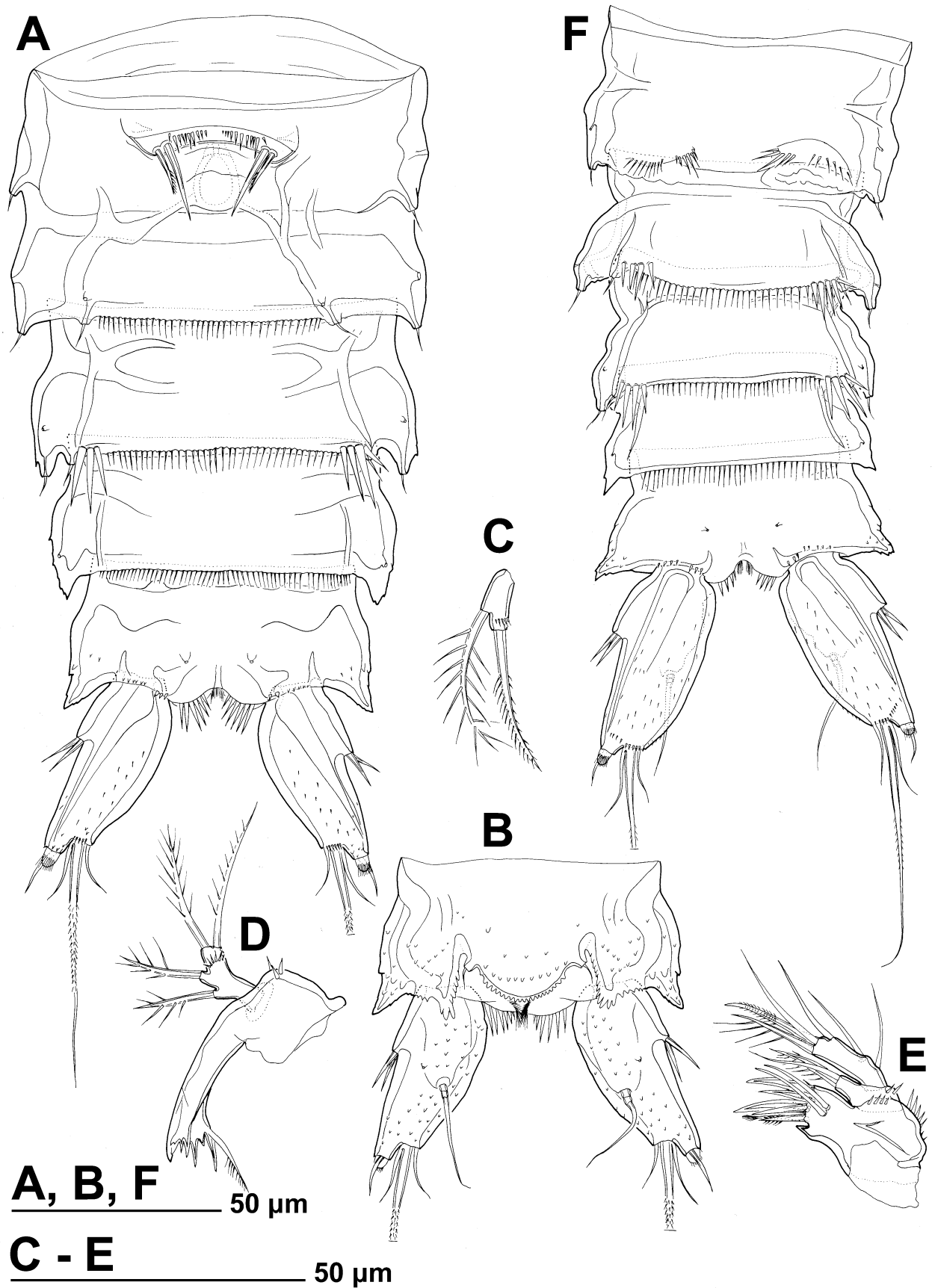
FIGURE 17. *Enhydrosoma kosmetron* **sp. nov.**, SEM photographs, A-C, paratype ♂2; D-H, paratype ♂3: A, habitus, ventral; B, maxilla, ventral; C, anal somite and caudal rami, ventral; D, rostrum and left antennula, ventral; E, antenna, ventral; F, mouth appendages, ventral; G, first swimming leg, anterior; H, fifth and sixth legs, anterior.
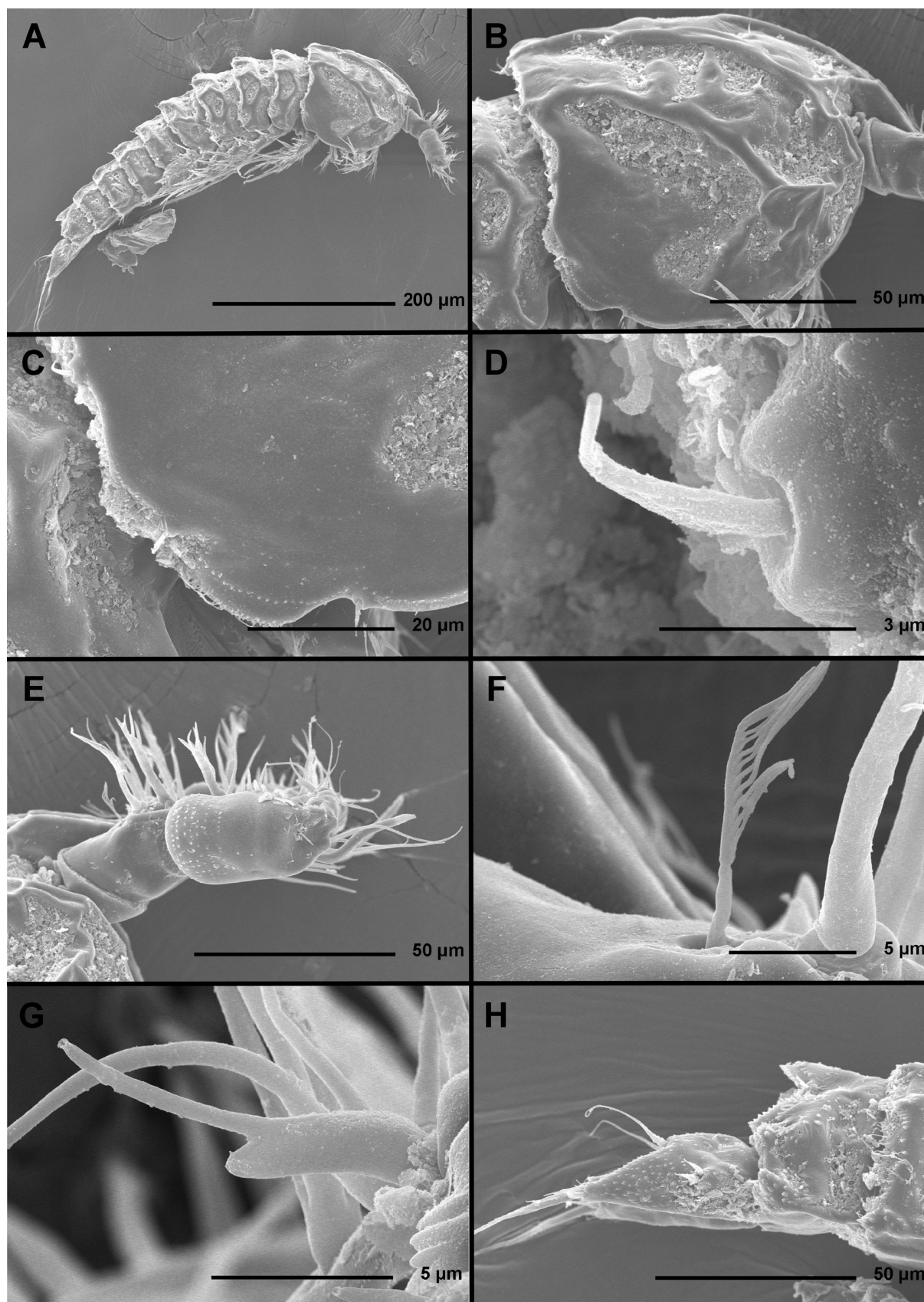
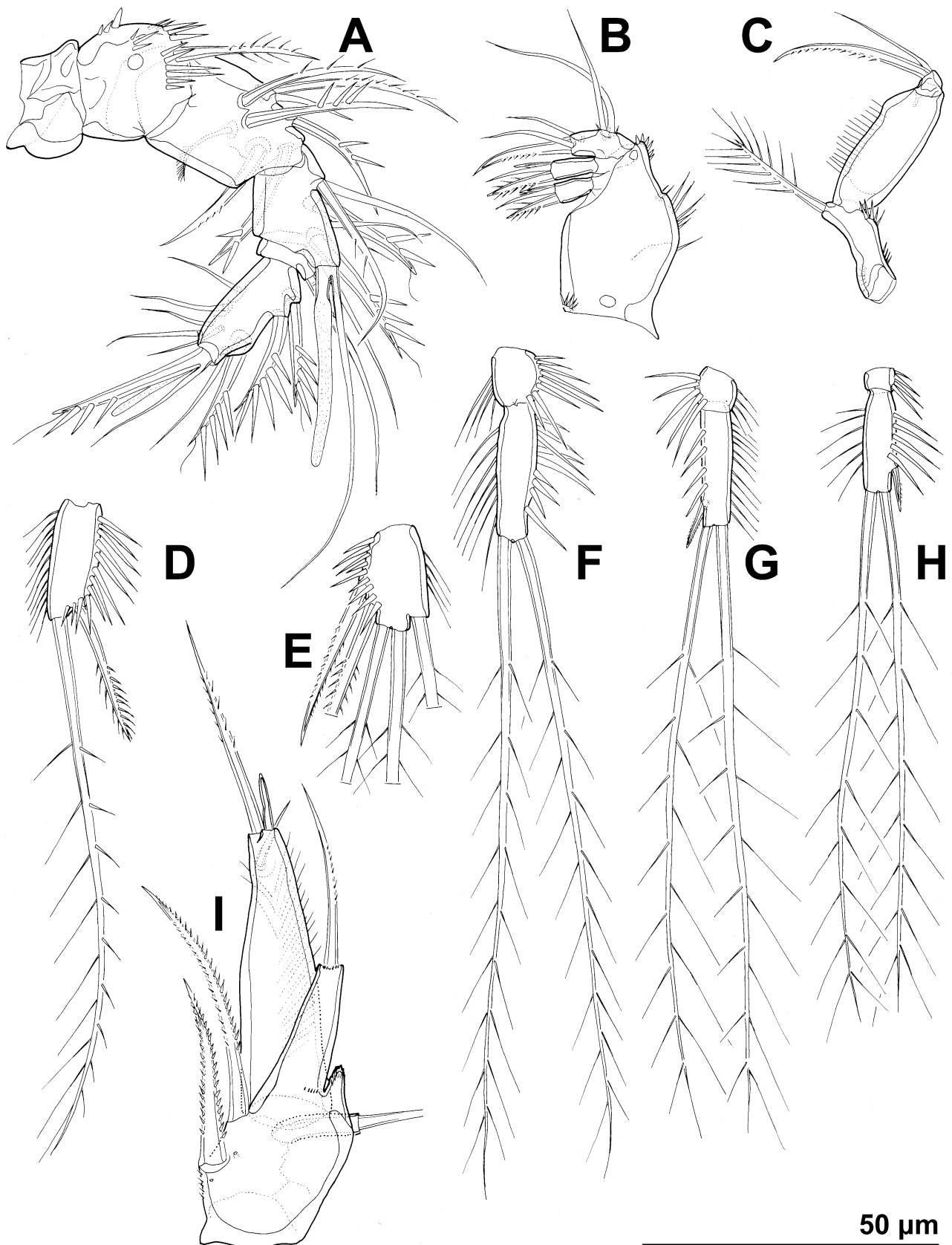**FIGURE 18.** *Enhydrosoma kosmetron* **sp. nov.**, SEM photographs, paratype ♂4: A, habitus, lateral; B, cephalic shield, lateral; C, postero-lateral corner of cephalic shield, lateral; D, sensillum on postero-lateral corner of cephalic shield; E, right antennula, lateral; F, transformed seta on first antennular segment, lateral; G, transformed seta on fifth antennular segment, lateral; H, anal somite and caudal rami, lateral.

FIGURE 19. *Enhydrosoma kosmetron* **sp. nov.**, line drawings, A-D, holotype ♀; F, allotype ♂: A, urosome, ventral; B, anal somite and caudal rami, dorsal; C, exopod of antenna, anterior; D, mandibula, posterior; E, maxillula, anterior; F, urosome, ventral.

FIGURE 20. *Enhydrosoma kosmetron* **sp. nov.**, line drawings, holotype ♀: A, antennula, ventral; B, maxilla, posterior; C, maxilliped, posterior; D, second endopodal segment of first leg, anterior; E, third exopodal segment of first leg, anterior; F, endopod of second leg, anterior; G, endopod of third leg anterior ; H, endopod of fourth leg, anterior; I, fifth leg, anterior.
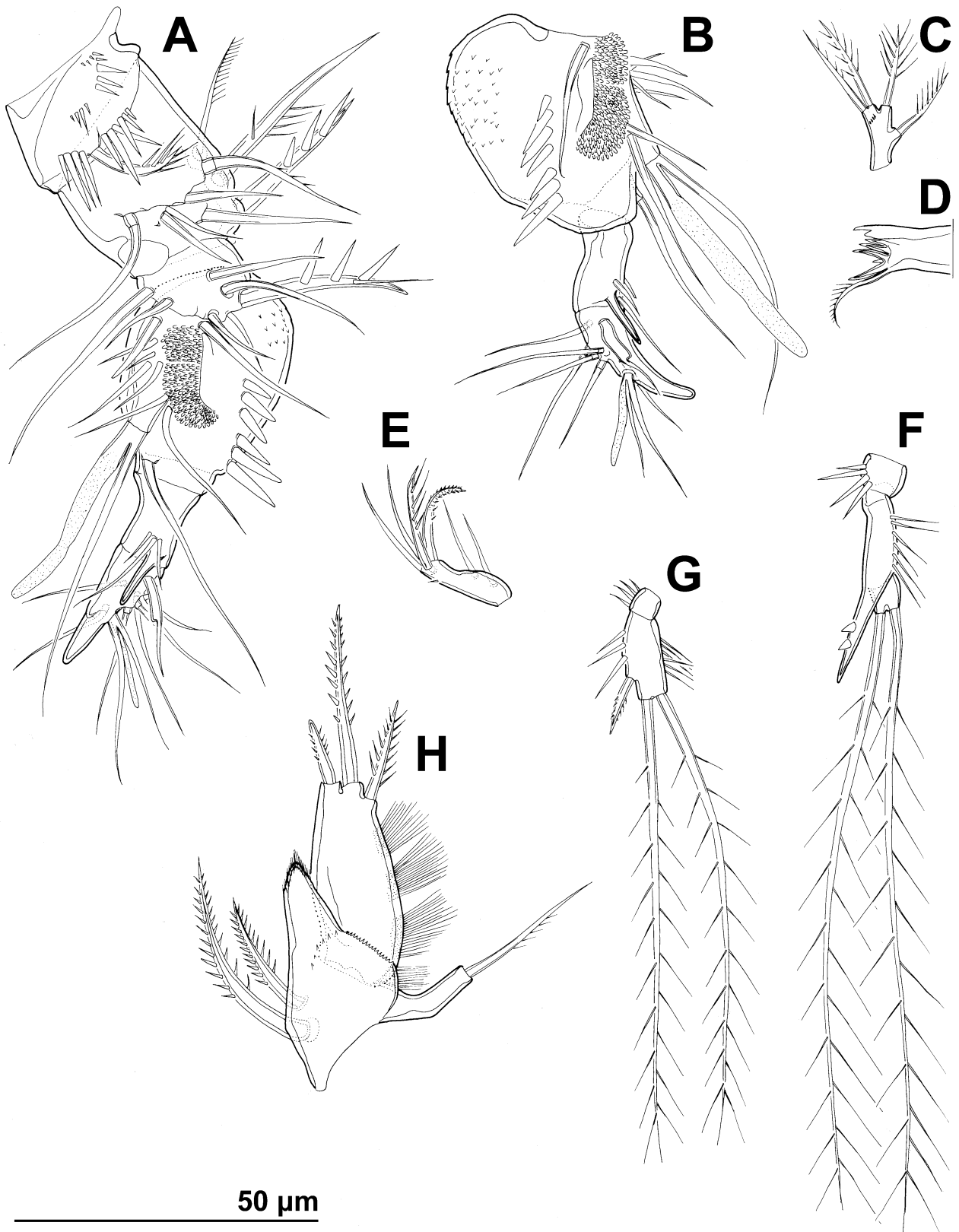
FIGURE 21. *Enhydrosoma kosmetron* **sp. nov.**, line drawings, allotype ♂: A, right antennula, ventral; B, distal part of left antennula, antero-ventral; C, mandibular palp, posterior; D, cutting edge of mandibula, posterior; E, maxillular palp, dorsal; F, endopod of third leg, anterior; G, endopod of fourth leg, anterior; H, fifth leg, anterior.

Third urosomite (Figs. 17H, 19F) as posterior part of genital double-somite in female but proportionately narrower, and with four or five large ventro-lateral spinules.

Caudal rami (Figs. 16H, 17C, 19F) very similar to those in female but slightly longer in proportion to anal somite and more robust.

Antennula (Figs. 17D, 18E, F, G, 21A, B) as in *E. apimelon*, except for second segment with two spiniform setae, third segment with one spiniform seta, fourth segment with large broom-like structure instead of brush and with only six or seven large spinules, fifth segment with large spiniform process and three slender setae, and sixth segment with large characteristically shaped tube pore (Fig. 18G); second segment as in female with slender plumose seta inserted into cone-like depression (Fig. 18F).

Endopod of third swimming leg (Fig. 21F) transformed and apparently three-segmented, with outer spine fused to segment and enlarged, secondary segmentation resulting in very small third segment bearing two long and slender apical setae.

Fifth leg (Figs. 17H, 21H) somewhat smaller than in female but with similar basic structure; exopod about 2.3 times as long as wide, with all three elements present and of similar proportions as in female, except for apical one bipinnate; endopodal lobe without distal armature element or inner spiniform processes, its distal tip with bunch of hair-like spinules; proximal endopodal inner spine about 1.6 times as long as distal endopodal inner spine and 1.2 times as long as longest element on exopod.

Sixth legs (Figs. 17H, 19F) as in *E. robustum*, withsimple cuticular plates, unarmed, with transverse row of slender spinules.

Variability. Despite numerous examined specimens and detailed examination using SEM (see Figs. 16A, G, 17A, 18A), we are not able to report on any significant morphological variability. The number of ventro-lateral spinules on fourth male and female urosomite and third male urosomite varies between three and five.

Molecular phylogeny

DNA was extracted and the mtCOI fragment successfully PCR-amplified from 14 cletodid copepod specimens (Table 1), belonging to six different morpho-species. Fragments ranged in length from 516 to 679 base pairs. All the sequences were translated into protein using MEGA and were shown to have no evidence of stop codons, ambiguities or insertions–deletions indicative of non-functional copies of mtCOI. BLAST analyses of GenBank revealed that the obtained sequences are copepod in origin and not contaminants.

Average pairwise distances between morpho-species were found to be very high (Table 2), all in excess of 22 %, suggesting only a relatively remote relationship between the studied taxa. These high divergence values are certainly indicative of distinct species by comparison with other crustaceans (Lefébure *et al.* 2006; Karanovic & Krajicek 2012a, b; Hamrova *et al.* 2012). The divergences between the three cletodid genera studied were also very high, ranging between 31.8 % and 38.4 %, and are comparable to those among some well accepted harpacticoid genera of the families Canthocamptidae, Parastenocarididae, and Miraciidae (Karanovic & Cooper 2011a, b, 2012; Karanovic *et al.* 2014; Karanovic & Kim 2014a, b). The highest average pairwise distance (38.4 %) was observed between *Geehydrosoma intermedia* and *Enhydrosoma robustum*, which is even higher than that between the genera *Stylicletodes* and *Geehydrosoma* (36.9 %). This is surprising considering that *Geehydrosoma intermedia* was until recently a member of the genus *Enhydrosoma* (see Introduction section and Kim *et al.* 2014), and it could be interpreted as an independent line of empirical data supporting the validity of these two genera. The highest average pairwise divergence between *Enhydrosoma* species was observed between *E. robustum* and *E. kosmetron* (30.8 %), while the lowest was observed between *E. kosmetron* and *E. coreana* (22.9 %).

The highest average divergences within morpho-taxa were those between three specimens of *E. coreana* (1.4 %), all from the same sampling location in Korea (St. 10; Table 1) and collected on the same date. Divergences between three specimens of *E. apimelon*, which also all came from the same sampling locality, but one was collected on a different occasion, are somewhat smaller (0.9 %). Divergences between three specimens of *G. intermedia* from Korea were zero, while those between the Russian specimen of this species and Korean specimens were only 0.4 % (i.e. two nucleotides), averaging 0.2 %. Sequences of the only other species of which we had more than one specimen, two Korean specimens of *Stylicletodes* sp., showed also a 0.2 % divergence. These are all indicative of intraspecific variability (Lefébure *et al.* 2006; Karanovic & Cooper 2011a, 2012).

TABLE 2. Average pairwise maximum likelihood distances (K2P model) among mtCOI sequences between each morpho-species (lower diagonal) and within morpho-species (diagonal). See text for authors of the specific names.

Species	1	2	3	4	5	6
1. *Enhydrosoma apimelon*	0.009					
2. *Enhydrosoma coreana*	0.250	0.014				
3. *Enhydrosoma kosmetron*	0.245	0.229	–			
4. *Enhydrosoma robustum*	0.290	0.257	0.308	–		
5. *Geehydrosoma intermedia*	0.340	0.355	0.318	0.384	0.002	
6. *Stylicletodes* sp.	0.336	0.339	0.340	0.352	0.369	0.002

All analyses (Fig. 22) supported the presence of at least six highly divergent lineages, and all four of the multi-sample lineages were supported with highest possible bootstrap values in all three analyses (100 %). The tree topology was the same in all three analyses as well, except in one of nine equally parsimonious trees in our MP analysis (all with a length of 449 steps, and only difference among the other eight trees in the exact intraspecific relationships). However, the bootstrap support values for basal nodes were different. The most terminal clade, suggesting a sister relationship of *E. coreana* and *E. robustum,* was moderately supported in our NJ and ML analyses (59 and 52 % respectively) but only weakly supported in our MP analysis (36 %). The clade suggesting a sister relationship of *E. apimelon* and the *E. coreana/E. robustum* clade was weakly supported in all our analyses (41 % in ML and only 33 % in MP and NJ analyses). Monophyly of the genus *Enhydrosoma* was moderately supported (79 % in NJ, 67 % in ML, and only 45 % in MP) but was recovered in all analyses even before tree rooting. This low support for the basal nodes could be explained by the low phylogenetic resolution of the mtCOI, possibly due to saturation at third codon positions (Karanovic & Cooper 2012), and only future analysis of some slower evolving genes may shed more light on this problem. Including more specimens and wider taxon sampling might be helpful as well, even though there is no evidence in our analyses for long branch attraction.
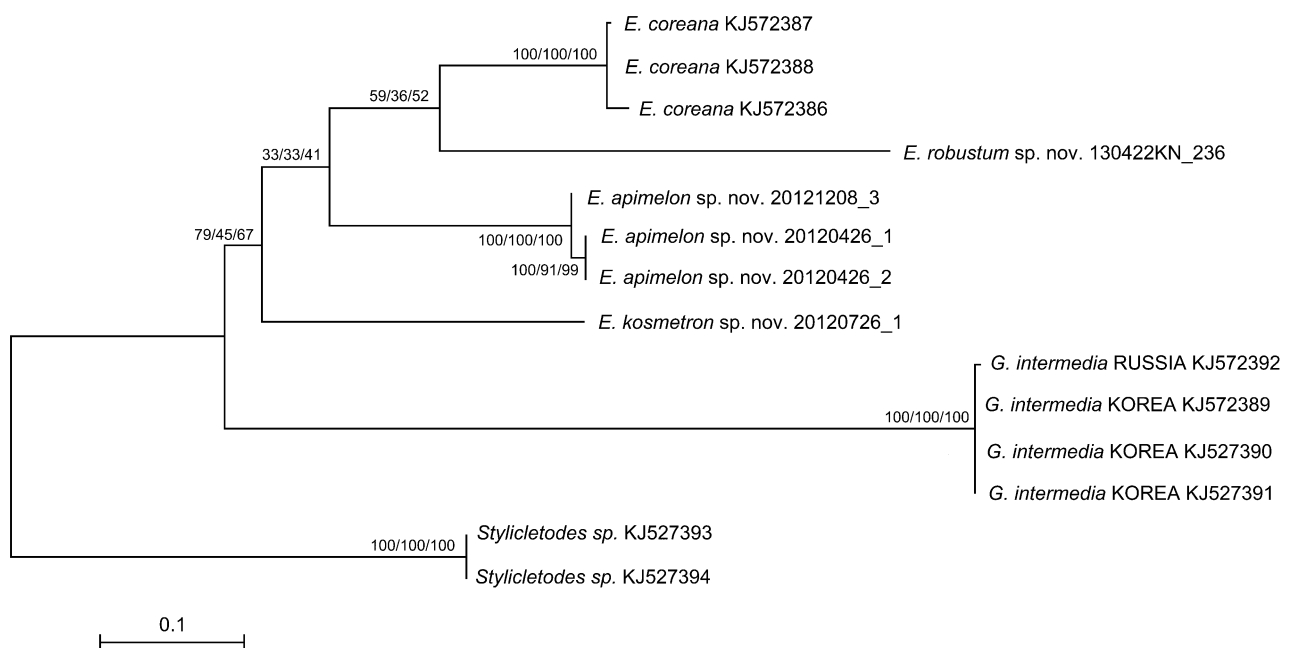
FIGURE 22. ML tree based on partial mtCOI sequence data from 14 Cletodidae specimens from Korea and Russia, constructed using MEGA v. 6 and TN93+G+I model of evolution, with numbers on branches representing NJ/MP/ML bootstrap values from 1000 pseudoreplicates. Cladogram is drawn to scale and specimen codes or GenBank numbers correspond to those in Table 1. MP values are those from last of nine equally parsimonious trees. All trees were rooted with *Stylicletodes* sp.

Morphology-based phylogeny

In addition to four endemic Korean *Enhydrosoma* species, we sampled morphological characters for this analysis also from the type species of this genus, *E. curticauda*, as re-described by Gee (1994), as well as from *Geehydrosoma intermedia* (Chislenko, 1978). The latter was recently separated from the genus *Enhydrosoma* by Kim *et al.* (2014), and re-described both from its type locality in Russia and from Korea. We used it as the outgroup for our analysis.

For this analysis the following 32 characters were selected, with character states in brackets (note: NONA requires characters to start from 0, rather than 1; somites and appendages are listed from anterior to posterior end of the body and character states were coded without a priori hypothesizing their apomorphic or plesiomorphic nature; all characters, except one, are binary, and that one is non-additive):

0. Rostrum: triangular (0); bifid (1).
1. Cephalic shield, ventral margin: smooth (0); with hair-like spinules (1); with ventral flaps (2).
2. Pleurons, pronounced dorso-lateral ridges: present (0); absent (1).
3. Prosomites, angle between telescopic and non-telescopic part: wide (0); sharp (1).
4. Anal operculum reaching beyond posterior margin: yes (0); no (1).
5. Caudal rami, dorsal seta position: central or posterior (0); anterior (1).
6. Caudal rami, proximal lateral setae position: anterior (0); posterior (1).
7. Caudal rami, distal lateral seta position: central (0); terminal (1).
8. Antennula in female, second segment, spiniform seta: absent (0); present (1).
9. Antennula in female, third segment, spiniform seta: absent (0); present (1).
10. Antennula in male, fourth segment, broom-like structure: absent (0); present (1).
11. Antennula in male, fifth segment, spiniform process: absent (0); present (1).
12. Antennula in male, sixth segment, large tubular pore: absent (0); present (1).
13. Mandibula, palp, number of armature elements: four (0); three (1).
14. Maxillula, palp: two-segmented (0); one-segmented (1).
15. Maxilliped, coxa, spinules: present (0); absent (1).
16. Maxilliped, coxa, seta: present (0); absent (1).
17. Maxilliped, endopod, slender seta exceeding midlength of spine: yes (0); no (1).
18. First swimming leg, third exopodal segment, number of elements: five (0); four (1).
19. First swimming leg, second endopodal segment, number of elements: three (0); two (1).
20. Third and fourth swimming legs, endopod, outer spine: present (0); absent (1).
21. Third swimming leg, endopod sexually dimorphic: yes (0); no (1).
22. Fifth leg in male and female, endopodal lobe longer than exopod: no (0); yes (1).
23. Fifth leg in female, tubular pores: absent (0); present (1).
24. Fifth leg in female, exopod, number of armature elements: four (0); three (1).
25. Fifth leg in male, exopod, number of armature elements: three (0); two (1).
26. Fifth leg in female, exopod, shape: wider proximally than distally (0); rectangular (1).
27. Fifth leg in female, exopod, innermost element: longest (0); shorter than next (1).
28. Fifth leg in male and female, endopodal lobe: short (0); produced posteriorly (1).
29. Fifth leg in female, endopodal lobe, spiniform projections: absent (0); present (1).
30. Sixth leg in female, number of armature elements: two (0); one (1).
31. Sixth leg in male, active genital operculum: left (0); right (1).

A character matrix was constructed (Table 3) to contain all character states for all species. Of the 32 characters used ten were uninformative (31%), which is not surprising considering that there are only five ingroup taxa. This proportion will undoubtedly drop as more taxa are added in the future. We refrained here from including any additional taxa for which we did not have molecular data (except the type species *E. curticauda*, as explained above). Seven of these ten uninformative characters are actually differences between the ingroup and outgroup, which belong to two different genera (characters no. 0, 7, 9, 14, 16, 28, and 30). They may play a more important role in subsequent broader phylogenetic analyses, and we did not see a reason to exclude them, as they cannot influence the tree topology at all. Two of the ten uninformative characters were autapomorphies of *E. apimelon* (characters no. 15 and 30) and one was an autapomorphy of *E. kosmetron* (character no. 18).
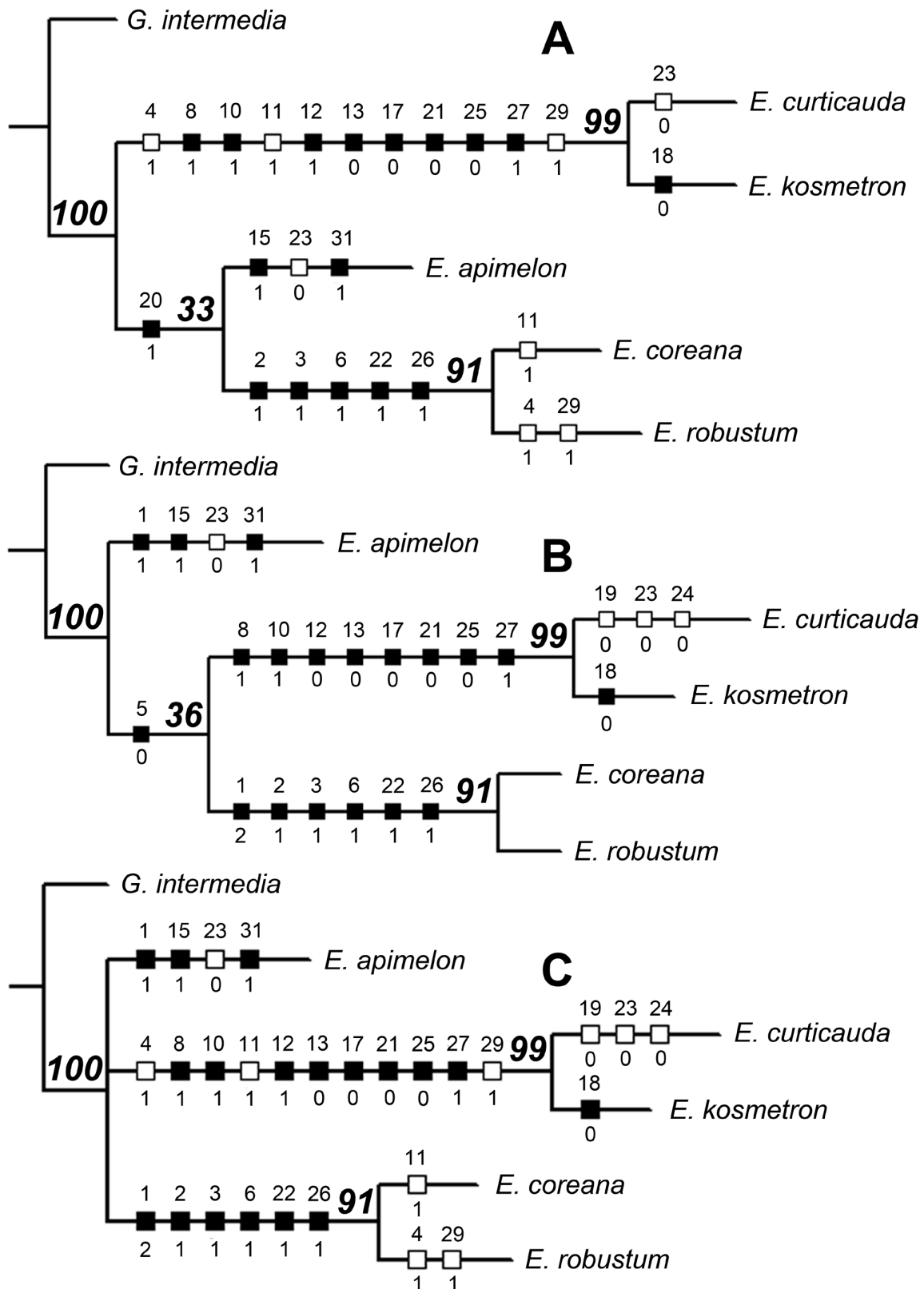
FIGURE 23. MP cladograms resulting from an analysis of 32 morphological characters (Table 3), scored for five *Enhydrosoma* Boeck, 1873 species and one outgroup, *Geehydrosoma intermedia* (Chislenko, 1978), constructed using Winclada/NONA and Rachet Island search method: A & B, two equally parsimonious trees; C, their strict consensus. Full squares represent presumed synapomorphies, empty squares represent presumed plesiomorphies or homoplasies, numbers above squares represent characters, numbers below squares represent character states, and large italic numbers on branches represent bootstrap values from 1000 pseudoreplicates.

TABLE 3. Character matrix for morphology-based cladistics analysis. See list of characters above for further explanation on character scoring.

Species\Characters	0	1	2	3	4	5	6	7	8	9	10	1	2	3	4	5
E. apimelon	1	1	0	0	0	1	0	1	0	1	0	0	0	1	0	1
E. coreana	1	2	1	1	0	0	1	1	0	1	0	1	0	1	0	0
E. curticauda	1	0	0	0	1	0	0	1	1	1	1	1	1	0	0	0
E. kosmetron	1	0	0	0	1	0	0	1	1	1	1	1	1	0	0	0
E. robustum	1	2	1	1	1	0	1	1	0	1	0	0	0	1	0	0
G. intermedia	0	0	0	0	0	1	0	0	0	0	0	0	0	1	1	0

continued.

Species\Characters	6	7	8	9	20	1	2	3	4	5	6	7	8	9	30	1
E. apimelon	0	1	1	1	1	1	0	0	1	1	0	0	1	0	0	1
E. coreana	0	1	1	1	1	1	1	1	1	1	1	0	1	0	0	0
E. curticauda	0	0	1	0	0	0	0	0	0	0	0	1	1	1	0	0
E. kosmetron	0	0	0	1	0	0	0	1	1	0	0	1	1	1	0	0
E. robustum	0	1	1	1	1	1	1	1	1	1	1	0	1	1	0	0
G. intermedia	1	1	1	0	0	1	0	1	0	1	0	0	0	0	1	0

Our cladistics analysis with all characters unweighted resulted in two equally parsimonious trees (Fig. 23A, B), with a length of 40 steps, a consistency index (Ci) of 0.82, and a retention index (Ri) of 0.73. Their strict consensus (Fig. 23C) resulted in one branch collapsing, and was one step longer, with a Ci of 0.8, and a Ri of 0.69. The values of the Ci and Ri indices indicate a significant proportion of convergences (homoplastic changes). This is obviously a result of the character choice and taxon sampling (including our outgroup choice), but it also reflects a general trait within harpacticoids, which is a high proportion of convergencies within almost any of its groups. However, the Ci and Ri indices are not nearly as low in this analysis of marine benthic species as they are in some subterranean freshwater harpacticoids (see Karanovic 2010; Karanovic & Lee 2012; Karanovic *et al.* 2013), and are even better than those in a group of also benthic marine species of the subfamily Stenheliinae Brady, 1880 (family Miraciidae Dana, 1846) analyzed recently by Karanovic & Kim (2014a). The ingroup is well defined and supported with maximum bootstrap values in all cladograms.

Topology of the first tree (Fig. 23A) is actually the same as that obtained for our molecular data, with the exclusion of *E. curticauda* for which we did not have any material for examination. It suggests as a terminal clade a sister relationship between *E. coreana* and *E. robustum*, which has a high boostrap support (91 %) and is based on five synapomorphies (characters no. 2, 3, 6, 22, and 26). Note that they combine morphological features of pleurons (which have rarely been studied in detail so far) and those of the caudal rami and fifth leg (both of which have been explored relatively well in previous studies). This terminal clade was also supported in the other two cladograms (Fig. 23B, C). All cladograms also support very strongly a sister relationships between *E. curticauda* and *E. kosmetron*, with bootstrap vales close to maximal (99 %) and no less than eight clear synapomorphies (characters no. 8, 10, 12, 13, 17, 21, 25, and 27). They are also well distributed over the entire body, including morphological features of the antennula, mandibula, maxilliped, third swimming leg, and fifth leg. Note that this species pair shares a number of homplasies as well, which include the relative length of the anal operculum, presence of a spiniform process on the male antennula, and presence of spiniform processes on the female fifth leg (characters no. 4, 11, and 29 respectively). The first and last character states are shared with *E. robustum*, while the character no. 11 is shared with *E. coreana*. It is difficult to estimate from our analysis if all of these are convergencies in a particular triplet or some may represent synapomorphies in a certain species pair, but it is symptomatic that all three characters are cuticular protrusions. This result may suggest a limited value of such characters in reconstructing phylogenetic relationships, at least in this group of copepods.

Our first cladogram (Fig. 23A) suggested *E. apimelon* as a sister clade to the *E. coreana*/*E. robustum* clade, as in our molecular phylogeny (Fig. 22). However, as in our molecular phylogeny, this relationship was very weakly supported (only 33 %), with a single synapomorphy suggested (character no. 20), i.e. absence of an outer spine on

endopods of the third and fourth legs. This simple reduction may have arisen convergently in at least one of these three species, and our alternative equally parsimonious tree (Fig. 23B) in fact suggests *E. apimelon* as a basal clade in our ingroup (albeit with a very low bootstrap support of 36 %). The strict consensus (Fig. 23C) of these two trees is an unresolved comb, suggesting that *E. apimelon* is only distantly related to the other four congeners studied here.

One of the more interesting results of this analysis is that characters such as the number of armature elements on the terminal endopodal segment of the first leg (character no. 19), as well as the presence of tubular pores on the fifth leg (character no. 23), and number of armature elements on the fifth leg exopod (character no. 24) are clearly homoplastic. These characters have been widely employed in harpacticoid taxonomy to define supraspecific taxa.

Discussion

All three new species described here, along with *Enhydrosoma coreana* Kim, Trebukova, Lee & Karanovic 2014, described from Korea, share a number of rare morphological features with the type species, *E. curticauda* (see Gee 1994). They include a strongly bifid rostrum with medially inserted sensilla, endopodal lobe of the fifth leg with a peduncle, and a characteristic shape of the female genital field. This type of rostrum is actually unique in the family, except perhaps in several species of *Kollerua* Gee, 1994 (see Borutzky 1928, Ranga Reddy 1979, Kikuchi *et al.* 1993). The fifth leg with a peduncle is only found in three species of the genus *Kollerua*, but this genus differs from *Enhydrosoma* by a number of morphological characters, most importantly by a one-segmented endopod of the fourth swimming leg. However, it is possible that the one-segmented condition of the endopod of the fourth leg may have arisen several times independently in cletodids, which would support the hypothesis about the polyphyletic nature of *Kollerua* (see Kim *et al.* 2014). Further support for this notion may be found in the very variable nature of the fifth leg in this genus, but this is beyond the scope of our study and would require molecular data and re-description of several species to be tested properly.

Therefore, it is quite plausible that the four Korean species and *E. curticauda* form a monophyletic group, which was one of the main reasons for exploring their phylogenetic relationships in this paper (see above). All four Korean species could easily be distinguished from each other by the shape of their caudal rami, which are short and conical in *E. coreana* (see Kim *et al.* 2014), long and slender in *E. apimelon* **sp. nov.** (see Fig. 2B), long and extremely robust in *E. robustum* **sp. nov.** (see Fig. 11B), and long and conical in *E. kosmetron* **sp. nov.** (see Fig. 16H). Probably partly as a consequence of their differently shaped caudal rami, the exact placement of certain caudal setae is different as well. For example, the dorsal seta is inserted more or less centrally in *E. coreana* and *E. kosmetron*, while it is inserted in the anterior half in *E. apimelon*, and in the posterior half in *E. robustum*. All four species could also be easily distinguished by the ornamentation of their male antennulae, which bare a large broom-like structure on their fourth segment in *E. kosmetron* (Fig. 17D), two thin combs in *E. robustum* (Fig. 13E), a small brush-like structure in *E. apimelon* (Fig. 4E), or nothing at all in this place in *E. coreana*. This appendage also has a different armature formula and some other differences in spiniform processes etc. (see above). Interspecific differences in the female caudal rami shape, armature, and ornamentation, as well as those in the male antennulae shape and ornamentation, make a lot of sense for species recognition among congeners that live sympatrically in environments with restricted optical and chemical conductivity (*Enhydrosoma* species are mud burrowers; see above), as was demonstrated already using a combined approach in the family Miraciidae by Karanovic & Cooper (2012) and Karanovic & Kim (2014b). These organs are used to lock a male and a female *in copula* in the first phase of the reproductive behavior in a majority of harpacticoids (see Huys & Boxshall 1991; Glatzel & Schminke 1996).

The four Korean *Enhydrosoma* species differ additionally in the relief pattern of their somites (note the unique triangular plates in *E. apimelon* in Fig. 3C), length of the anal operculum (very short in *E. robustum*; see Fig. 14B), ornamentation of urosome, and especially in the exact shape, armature, and ornamentation of the fifth leg (compare, for example, Figs. 6J, 15H, I, and 20I; these appendages are extensively exploited for scoring characters for our morphology-based phylogenetic analysis above). Several additional minor differences are pointed out between the three new species in their comparative descriptions above and also highlighted by arrows in some figures. *Enhydrosoma kosmetron* differs from the other three species also by the armature of mandibula (Fig. 19D) and some swimming legs (Fig. 20E, G, H). However, this species shares almost all of the above mentioned morphological features with the European *E. curticauda*, including the shape and ornamentation of all somites and

caudal rami, ornamentation and armature of the antennula both in male and female, and the sexually dimorphic endopod of the third leg. There is no doubt that *E. kosmetron* and *E. curticauda* represent a sister-species pair among currently known congeners, as it would be impossible to imagine all that fine ornamentation and complicated structures originating convergently. However, it is interesting that they differ in characters that are often used to define supraspecific taxa in harpacticoid taxonomy (see Lang 1948, 1965 for example), such as the number of setae on the first leg endopod and the fifth leg exopod (*E. curticauda* has one additional seta on each). *Enhydrosoma curticauda* differs additionally from *E. kosmetron* by the presence of tubular pores on the fifth leg, as well as by the slightly shorter caudal rami. All four Korean species differ from other congeners by a great number of morphological features, and are probably only remotely related to them, adding pressure for the long overdue revision of this genus (Gee 1994; Kim *et al.* 2014).

Congruence between our molecular and morphology-based phylogenies (see above), even though based on a small number of taxa, may help to encourage such revision and point out both useful and not-so-useful morphological characters for defining supraspecific groups. Not surprisingly, the sister-species relationship between *E. kosmetron* and *E. curticauda* was recovered and supported with high bootstrap values in all our morphology-based cladograms (Fig. 23), and it is unfortunate that we could not obtain any fresh material for our molecular analysis. This certainly remains one of the priorities for our future studies, along with a wider taxon sampling. The fact that *E. coreana* and *E. robustum* are suggested as sister species in our molecular and morphological analyses (Figs. 22, 23) gives us additional confidence in our choice of morphological characters. Our molecular cladograms, and even some of our morphology-based cladograms (Figs 22, 23A) suggest *E. apimelon* as a sister clade to the terminal *E. coreana/E. robustum* clade, but that relationship had a weak bootstrap support in all analyses and is something that cannot be resolved without a wider taxon and character sampling (including additional molecular markers). Characters supporting each of these clades are discussed above.

It is worth repeating here that our ingroup was well supported in all analyses, suggesting a monophyly of these five *Enhydrosoma* species. Although the four Korean species slightly bridge the gap between the type species and other congeners, these five still have a very isolated position within the genus. Most of the morphological differences are in fact synapomorphies of these five species, which would make it easy to separate them from other congeners. However, as one of them is the type species of *Enhydrosoma,* all other members would have to be transferred into a newly erected genus. This would only perpetuate the problem of supporting extremely heterogeneous groups (see above), and we feel reluctant to attempt any such revision without the use of molecular data and re-description of species that are inadequately described.

For example, a re-examination of the holotype and newly collected material from and near the type locality of *E. intermedia* by Kim *et al.* (2014) showed that several features described and illustrated by Chislenko (1978) were not correct. These inaccuracies and the lack of known males probably prevented Gómez (2004) from noticing a very close relationship between this Russian Far Eastern species and his new species from the Pacific coast of Mexico (*E. brevipodum* Gómez, 2004). In addition to re-describing the female of *E. intermedia,* Kim *et al.* (2014) also described the male of that species for the first time and erected a new genus (*Geehydrosoma* Kim *et al.*, 2014) to accommodate it and the Mexican congener. Interestingly, these two species, just like *E. kosmetron* and *E. curticauda*, share many morphological features down to minute details of ornamentation of somites and caudal rami but differ mostly in the relative length of their caudal rami. The distribution of the genus *Geehydrosoma* in the Northern Pacific makes a lot of sense when trying to imagine dispersal routes of the presumed immediate ancestor of its two congeners. Similarly, an immediate common ancestor of the *E. curticauda/E. kosmetron* sister-species pair may have had a wide Euro-Asian distribution, with the present disjunct distribution probably being caused by the Cenozoic temperature drop and freezing of the Arctic Sea.

Even though the five species of *Enhydrosoma* analyzed above form a monophyletic group, their very high divergence values (Table 2) suggest that they are not very closely related and that all divergence times probably predate any Cenozoic climatic oscillations. We base this interpretation on some recent molecular work which showed comparable divergences in the same gene between some well-established genera in three different harpacticoid families. Karanovic & Cooper (2011b) showed divergences among tree genera of the family Parastenocarididae Chappuis, 1940 to be in excess of 22 %, Karanovic & Cooper (2012) similarly showed divergences among three genera of the family Canthocamptidae Brady, 1880 to be in excess of 27 %, and Karanovic & Kim (2014a) showed divergences among six genera of the family Miraciidae Dana, 1846 to be between 17 and 38 %.

A very small divergence value between the Russian and Korean specimens of *G. intermedia* (0.4 %) shows that these animals have a significant dispersal potential, as the divergences are much smaller than those observed among specimens of *E. apimelon* (0.9 %) or *E. coreana* (1.4 %) collected from the same locality in Korea (see Table 2). We believe that the disjunct distribution of *G. intermedia*, that spans more than 1200 km of coastline, is a consequence of a natural long-distance dispersal and not anthropogenic translocation (see Karanovic & Krajicek 2012a), as the Korean population is homogenous genetically and morphologically (see Kim *et al.* 2014) and it differs from the Russian population in two nucleotides.

Although it is quite clear that many morphological synapomorphies define our ingroup, at this stage we can only speculate on where the bulk of *Enhydrosoma* species would nest between it and the genus *Geehydrosoma*. The absence of sexual dimorphism on the male P3 endopod was recorded in at least ten other species of *Enhydrosoma* (see Gómez 2004) and several other genera of cletodids, a recurved and enlarged outer spine on the male P3 second exopodal segment was reported for three species (*E. gariene* Gurney, 1930; *E latipes* (A. Scott, 1909); *E. pericoense* Mielke, 1990), a maxilliped lacking a syncoxal seta was observed in more than ten species (Gee 1994), and a one-segmented maxillular palp with only five setae was reported in at least ten species (Lang 1948, Raibaut 1965, Wells 1967, Bell & Kern 1983, Mielke 1990, Gee 1994, Gómez 2003). While some of these characters (and others not mentioned here) may have originated convergently (especially those involving reduced armature), it is possible that at least some of them have a broader phylogenetic value and should be used in future phylogenetic studies. Unfortunately, many characters that showed a great phylogenetic value in our analyses above, such as those of the somite and antennula ornamentation, are unknown for most *Enhydrosoma* species.

References

Bell, S.S. & Kern, J.C. (1983) A new species of *Enhydrosoma* (Copepoda, Harpacticoida) from Tampa Bay, Florida. *Florida Bulletin of Marine Science*, 33, 899–904.

Bláha, M., Hulák, M., Slouková, J. & Těšitel, J. (2010) Molecular and morphological patterns across *Acanthocyclops vernalis-robustus* species complex (Copepoda, Cyclopoida). *Zoologica Scripta*, 39, 259–268.
http://dx.doi.org/10.1111/j.1463-6409.2010.00422.x

Borutzky, E.W. (1928) *Enhydrosoma uniarticulatum* sp. nov. (Copepoda, Harpacticoida), ein neuer Vertreter der Gattung *Enhydrosoma. Zoologischer Anzeiger*, 80, 158–160.

Boxshall, G.A. & Halsey, S.H. (2004) *An Introduction to Copepod Diversity.* The Ray Society, London, 966 pp.

Burgess, R. (2001) An improved protocol for separating meiofauna from sediments using colloidal silica soils. *Marine Ecology Progress Series*, 214, 161–165.
http://dx.doi.org/10.3354/meps214161

Chislenko, L.L. (1978) New species of harpacticoid copepods (Copepoda, Harpacticoida) from Posyet Bay, Sea of Japan. *Trudy Zoologicheskogo Instituta, Akademii Nauk SSSR, Leningrad*, 61, 161–192. [in Russian]

Fiers, F. (1987) *Enhydrosoma vervoorti* spec. nov., a new harpacticoid copepod from India (Harpacticoida: Cletodidae*). Zoologische Mededelingen*, 61, 295–302.

Fiers, F. (1996) Re-description of *Enhydrosoma lacunae* Jakubisiak, 1933 (Copepoda, Harpacticoida), with comments on the *Enhydrosoma* species reported from West Atlantic localities, and a discussion of cletodid development. *Sarsia*, 81, 1–17.

Folmer, O., Black, M., Hoeh, W., Lutz, R. & Vrijenoek, R. (1994) DNA primers for amplification of mitochondrial cytochrome c oxidase subunit 1 from diverse metazoan invertebrates. *Molecular Marine Biology and Biotechnology*, 3, 294–299.

Gee, J.M. (1994) Towards a revision of *Enhydrosoma* Boeck, 1872 (Harpacticoida: Cletodidae *sensu* Por); a re-examination of the type species, *E. curticauda* Boeck, 1872, and the establishment of *Kollerua* gen. nov. *Sarsia*, 79, 83–107.

Gee, J.M. (2001) A reappraisal of the taxonomic position of *Enhydrosoma curvirostre* (Copepoda: Harpacticoida: Cletodidae). *Journal of the Marine Biological Association of the United Kingdom*, 81, 33–42.
http://dx.doi.org/10.1017/s002531540100337x

Gee, J.M. & Huys, R. (1996) An appraisal of the taxonomic position of *Enhydrosoma buchholzi* (Boeck, 1872), *E. bifurcarostrum* Shen & Tai, 1965, *E. barnishi* Wells, 1967 and *E. vervoorti* Fiers, 1987 with definition of two new genera (Copepoda, Harpacticoida, Cletodidae). *Sarsia*, 81, 161–191.

Glatzel, T. & Schminke, H.K. (1996) Mating behavior of the groundwater copepod *Parastenocaris phyllura* Kiefer, 1938 (Copepoda: Harpacticoida). *Contributions to Zoology*, 66, 103–108.

Goloboff, P. (1999) *NONA (NO NAME) Version 2.* Published by the author, Tucumán, Argentina.

Gómez, S. (2003) Three new species of *Enhydrosoma* and a new record of *Enhydrosoma lacunae* (Copepoda: Harpacticoida: Cletodidae) from the Eastern Tropical Pacific. *Journal of Crustacean Biology*, 23, 94–118.
http://dx.doi.org/10.1163/20021975-99990320

Gómez, S. (2004) A new species of *Enhydrosoma* Boeck, 1872 (Copepoda: Harpacticoida: Cletodidae) from Eastern Tropical Pacific. *Proceedings of the Biological Society of Washington*, 117, 529–540.

Guindon, S. & Gascuel, O. (2003) A simple, fast and accurate method to estimate large phylogenies by maximum likelihood. *Systematic Biology*, 52, 696–704.
http://dx.doi.org/10.1080/10635150390235520

Hamrova, E., Krajicek, M., Karanovic, T., Cerny, M. & Petrusek, A. (2012) Congruent patterns of lineage diversity in two species complexes of planktonic crustaceans, *Daphnia longispina* (Cladocera) and *Eucyclops serrulatus* (Copepoda), in East European mountain lakes. *Zoological Journal of the Linnean Society*, 166, 754–767.
http://dx.doi.org/10.1111/j.1096-3642.2012.00864.x

Hebert, P.D.N., Cywinska, A., Ball, S.L. & deWaard, J.R. (2003) Biological identifications through DNA barcodes. *Proceedings of the Royal Society of London*, 270, 313–321.
http://dx.doi.org/10.1098/rspb.2002.2218

Huys, R. & Boxshall, G.A. (1991) *Copepod Evolution.* The Ray Society, London, 468 pp.

Huys, R., Fatih, F, Ohtsuka, S. & Llewellyn-Hughes, J. (2012) Evolution of the bomolochiform superfamily complex (Copepoda: Cyclopoida): New insights from ssrDNA and morphology, and origin of umazuracolids from polychaete-infesting ancestors rejected. *International Journal of Parasitology*, 42, 71–92.
http://dx.doi.org/10.1016/j.ijpara.2011.10.009

Huys, R., Llewellyn-Hughes, J., Conroy-Dalton, S., Olson, P.D., Spinks, J. & Johnston, D.A. (2007) Extraordinary host switching in siphonostomatoid copepods and the demise of the Monstrilloida: integrating molecular data, ontogeny and antennulary morphology. *Molecular Phylogenetics and Evolution*, 43, 368–378.
http://dx.doi.org/10.1016/j.ympev.2007.02.004

Huys, R., Llewellyn-Hughes, J., Olson, P.D. & Nagasawa, K. (2006) Small subunit rDNA and Bayesian inference reveal *Pectenophilus ornatus* (Copepoda *incertae sedis*) as highly transformed Mytilicolidae, and support assignment of Chondracanthidae and Xarifiidae to Lichomolgoidea (Cyclopoida). *Biological Journal of the Linnean Society*, 87, 403–425.
http://dx.doi.org/10.1111/j.1095-8312.2005.00579.x

Huys, R., MacKenzie-Dodds, J. & Llewellyn-Hughes, J. (2009) Cancrincolidae (Copepoda, Harpacticoida) associated with land crabs: a semiterrestrial leaf of the ameirid tree. *Molecular Phylogenetics and Evolution*, 51, 143–156.
http://dx.doi.org/10.1016/j.ympev.2008.12.007

Karanovic, T. (2010) First record of the harpacticoid genus *Nitocrellopsis* (Copepoda, Ameiridae) in Australia, with descriptions of three new species. *International Journal of Limnology*, 46, 249–280.
http://dx.doi.org/10.1051/limn/2010021

Karanovic, T. & Cooper, S.J.B. (2011a) Molecular and morphological evidence for short range endemism in the *Kinnecaris solitaria* complex (Copepoda: Parastenocarididae), with descriptions of seven new species. *Zootaxa*, 3026, 1–64.

Karanovic, T. & Cooper, S.J.B. (2011b) Third genus of paratenocaridid copepods from Australia supported by molecular evidence (Copepoda, Harpacticoida). *In:* Defaye, D., Suárez-Morales, E. & von Vaupel Klein, J.C. (Eds.), *Crustaceana Monographs, Studies on Freshwater Copepoda: a Volume in Honour of Bernard Dussart.* Brill, Nevada, 293–337.
http://dx.doi.org/10.1163/ej.9789004181380.i-566.116

Karanovic, T. & Cooper, S.J.B. (2012) Explosive radiation of the genus *Schizopera* on a small subterranean island in Western Australia (Copepoda : Harpacticoida): unravelling the cases of cryptic speciation, size differentiation and multiple invasions. *Invertebrate Systematics*, 26, 115–192.
http://dx.doi.org/10.1071/is11027

Karanovic, T., Eberhard, S.M., Perina, G. & Callan, S. (2013) Two new subterranean ameirids (Crustacea : Copepoda : Harpacticoida) expose weaknesses in the conservation of short-range endemics threatened by mining developments in Western Australia. *Invertebrate Systematics*, 27, 540–566.

http://dx.doi.org/10.1071/is12084

Karanovic, T. & Kim, K. (2014a) Suitability of cuticular pores and sensilla for harpacticoid copepod species delineation and phylogenetic reconstruction. *Arthropod Structure & Development*, 43, 615–658. http://dx.doi.org/10.1016/j.asd.2014.09.003

Karanovic, T. & Kim, K. (2014b) New insights into polyphyly of the harpacticoid genus *Delavalia* (Crustacea, Copepoda) through morphological and molecular study of an unprecedented diversity of sympatric species in a small South Korean bay. *Zootaxa*, 3783 (1), 1–96. http://dx.doi.org/10.11646/zootaxa.3783.1.1

Karanovic, T., Kim, K. & Lee, W. (2014) Morphological and molecular affinities of two East Asian species of *Stenhelia* (Crustacea, Copepoda, Harpacticoida). *ZooKeys*, 411, 105–143. http://dx.doi.org/10.3897/zookeys.411.7346

Karanovic, T. & Krajicek, M. (2012a) When anthropogenic translocation meets cryptic speciation globalised bouillon originates; molecular variability of the cosmopolitan freshwater cyclopoid *Macrocyclops albidus* (Crustacea: Copepoda). *International Journal of Limnology*, 48, 63–80. http://dx.doi.org/10.1051/limn/2011061

Karanovic, T. & Krajicek, M. (2012b) First molecular data on the Western Australian *Diacyclops* (Copepoda, Cyclopoida) confirm morpho-species but question size differentiation and monophyly of the *alticola*-group. *Crustaceana*, 85, 1549–1569. http://dx.doi.org/10.1163/156854012x651709

Karanovic, T. & Lee, W. (2012) A new species of *Parastenocaris* from Korea, with a re-description of the closely related *P. biwae* from Japan (Copepoda: Harpacticoida: Parastenocarididae). *Journal of Species Research*, 1, 4–34.

Kikuchi, Y., Dai, A.-Y. & Itô, T. (1993) Three species of harpacticoids (Crustacea, Copepoda) from Lake Tai-Hu, eastern China. *Publications of Itako Hydrobiological Station*, 6, 17–25.

Kim, K., Trebukhova, Y., Lee, W. & Karanovic, T. (2014) A new species of *Enhydrosoma* (Copepoda: Harpacticoida: Cletodidae) from Korea, with re-description of *E. intermedia* and establishment of a new genus. *Proceedings of the Biological Society of Washington*, 127, 248–283. http://dx.doi.org/10.2988/0006-324X-127.1.248

Kimura, M. (1980) A simple method for estimating evolutionary rate of base substitutions through comparative studies of nucleotide sequences. *Journal of Molecular Evolution*, 16, 111–120. http://dx.doi.org/10.1007/bf01731581

Lang, K. (1936) Die Familie der Cletodidae, Sars, 1909. *Zoologische Jahrbücher Systematik*, 68, 445–480.

Lang, K. (1948) *Monographie der Harpacticiden. 1-2.* Nordiska Bokhandeln, Lund, 1682 pp.

Lang, K. (1965) Copepoda Harpacticoida from the Californian Pacific coast. *Kungliga Svenska Vetenskapsakademiens Handlingar*, 10, 1–560.

Lee, C.E., Remfert, J.L. & Chang, Y.-M. (2007) Response to selection and evolvability of invasive populations. *Genetica*, 129, 179–192. http://dx.doi.org/10.1007/s10709-006-9013-9

Lee, C.E., Remfert, J.L. & Gelembiuk, G.W. (2003) Evolution of physiological tolerance and performance during freshwater invasions. *Integrative and Comparative Biology*, 43, 439–449. http://dx.doi.org/10.1093/icb/43.3.439

Lefébure, T., Douady, C.J., Gouy, M. & Gibert, J. (2006) Relationship between morphological taxonomy and molecular divergence within Crustacea: Proposal of a molecular threshold to help species delimination. *Molecular Phylogeny and Evolution*, 40, 435–447. http://dx.doi.org/10.1016/j.ympev.2006.03.014

Mielke, W. (1990) *Zausodes septimus* Lang, 1965 und *Enhydrosoma pericoense* nov. spec., zwei bentische Ruderfusskrebse (Crustacea, Copepoda) aus dem Eulitoral von Panamá. *Microfauna Marina*, 6, 139–156.

Nixon, K.C. (1999) The parsimony ratchet, a new method for rapid parsimony analysis. *Cladistics*, 15, 407–414. http://dx.doi.org/10.1006/clad.1999.0121

Nixon, K.C. (2002) *WinClada version 1.00.08.* Published by the author, Ithaca, New York.

Por, D. (1986) A re-evaluation of the family Cletodidae Sars, Lang, (Copepoda, Harpacticoida). *In:* Schriever, G., Schminke, H.K. & Shih, S.-T. (Eds.), *Proceedings of the Second International Conference on Copepoda, Ottawa, Canada, 13-17th August 1984, Syllogeus*, 58, 420–425.

Posada, D. & Crandall, K.A. (1998) Modeltest: testing the model of DNA substitution. *Bioinformatics*, 14, 817–818. http://dx.doi.org/10.1093/bioinformatics/14.9.817

Raibaut, A. (1965) Sur quelques Cletodidae (Copepoda, Harpacticoida) du Bassin de Thau. *Crustaceana*, 8, 113–120. http://dx.doi.org/10.1163/156854065x00631

Ranga Reddy, Y. (1979) *Enhydrosoma radhakrishnai* n. sp. (Copepoda, Harpacticoida) from Lake Kolleru, South India. *Crustaceana*, 36, 9–14. http://dx.doi.org/10.1163/156854079x00159

Sakaguchi, S.O. & Ueda, H. (2010) A new species of *Pseudodiaptomus* (Copepoda: Calanoida) from Japan, with notes on the closely related *P. inopinus* Burckhardt, 1913 from Kyushu Island. *Zootaxa*, 2612, 52–68.

Sars, G.O. (1909) *An account of the Crustacea of Norway. Vol. 5. Harpacticoida.* Bergen Museum, Bergen, 449 pp.

Stock, J.K. & von Vaupel Klein, J.C. (1996) Mounting media revisited: the suitability of Reyne's fluid for small crustaceans. *Crustaceana*, 69, 749–798.
http://dx.doi.org/10.1163/156854096x00826

Tamura, K. (1992) Estimation of the number of nucleotide substitutions when there are strong transition-transversion and G + C-content biases. *Molecular Biology and Evolution,* 9, 678–687.

Tamura, K., Stecher, G., Peterson, D., Filipski, A. & Kumar, S. (2013) MEGA6: Molecular Evolutionary Genetics Analysis Version 6.0. *Molecular Biology and Evolution*, 30, 2725–2729.
http://dx.doi.org/10.1093/molbev/mst197

Thompson, J.D., Higgins, D.G. & Gibson, T.J. (1994) CLUSTAL W: improving the sensitivity of progressive multiple sequence alignment through sequence weighting, position-specific gap penalties and weight matrix choice. *Nucleic Acids Research*, 22, 4673–4680.
http://dx.doi.org/10.1093/nar/22.22.4673

Walter, T.C. & Boxshall, G. (2015) World Copepoda database. Available from: http://www.marinespecies.org/copepoda (accessed on 10 January 2015)

Wells, J.B.J. (1967) The littoral Copepoda (Crustacea) of Inhaca Island, Mozambique. *Transactions of the Royal Society of Edinburgh,* 67,189–358.
http://dx.doi.org/10.1017/s0080456800024017

Wells, J.B.J. (2007) An annotated checklist and keys to the species of Copepoda Harpacticoida. *Zootaxa*, 1568, 1–872.

Winkler, G., Dodson, J.J. & Lee, C.E. (2008) Heterogeneity within the native range: population genetic analyses of sympatric invasive and noninvasive clades of the freshwater invading copepod *Eurytemora affinis. Molecular Ecology*, 17, 415–430.
http://dx.doi.org/10.1111/j.1365-294x.2007.03480.x

Wyngaard, G.A., Holynska, M. & Schulte, J.A. II (2010) Phylogeny of the freshwater copepod *Mesocyclops* (Crustacea: Cyclopidae) based on combined molecular and morphological data, with notes on biogeography. *Molecular Phylogenetics and Evolution*, 55, 753–764.
http://dx.doi.org/10.1016/j.ympev.2010.02.029

KARANOVIC *ET AL.*